

**Biomimetic nanocomposites of calcium phosphate and self-assembling triblock and pentablock copolymers**

by

**Drew Lenzen Enlow**

A thesis submitted to the graduate faculty  
in partial fulfillment of the requirements for the degree of

MASTER OF SCIENCE

Major: Materials Science and Engineering

Program of Study Committee:  
Mufit Akinc, Major Professor  
Surya Mallapragada  
Zhiqun Lin

Iowa State University

Ames, Iowa

2006

Graduate College  
Iowa State University

This is to certify that the master's thesis of

Drew Lenzen Enlow

has met the thesis requirements of Iowa State University

  
Major Professor

For the Major Program

## Table of Contents

<b>Acknowledgements</b>	iv
<b>Thesis Organization</b>	vi
<b>Abstract</b>	vii
<b>Chapter 1: General Introduction</b>	1
Background Information	2
Biological Inspiration	2
Calcium Phosphate	3
Synthetic Self-Assembling Block Copolymers as Templates	7
Organic-Inorganic Nanocomposite Materials	9
References	11
<b>Chapter 2: Biomimetic Calcium Phosphate Precipitation on Nanoscale Pentablock Polymer Micelles</b>	13
Introduction	14
Materials and Methods	18
Characterization	20
Results and Discussion	21
Conclusions	27
References	29
<b>Chapter 3: Preparation of Tri and Pentablock Polymer-Calcium Phosphate Gel Nanocomposites</b>	31
Introduction	32
Materials and Methods	35
Characterization	36
Results and Discussion	40
Conclusions	49
References	51
<b>Chapter 4: General Conclusions</b>	52
Summary	52
Conclusions	52
Future Research	53

## Acknowledgements

I would like to acknowledge my group members, collaborators, and other faculty and students who have helped me along the way. Yusuf Yusufoglu, Xiang Wei, Zhihong Tang, Matt Kramer, Andy Thom, and Shannon Dudley provided countless ideas and suggestions in group meetings and were always helpful whenever I needed anything. The expertise and technical support of Ozan Ugurlu, Eren Kalay, Umai Kanapathipillai, Tracey Pepper, Dr. Scott Chumbley, Adu Rawal, and Dr. Klaus Schmidt-Rohr was also invaluable.

It is my pleasure to thank the members of my program of study committee Dr. Zhiqun Lin, Dr. Surya Mallapragada, and especially my major professor Dr. Mufit Akinc. It was their guidance and wisdom that got me through this process.

Finally, I would like to dedicate this thesis to my family. None of this would have been possible without the moral and financial support given by my parents Keith and Marguerite Enlow. My parents as well as my brother, Jacob Enlow's encouragement and patience throughout my years at Iowa State have meant more to me than I ever realized. I also need to thank my closest friends. Alek Pochowski, Jake Nickel, Chad Smith, Ryan Meyer, Scott Williams, Matt Pitcher, and Emily Evers have made the past several years the best of my life.

The United States Government has assigned the DOE report IS-T 2820 to this thesis. Notice: This document has been authorized by the Iowa State University of Science and Technology

under Contract No. W-7405-ENG-82 with the U.S. Department of Energy. The U.S. Government retains a non-exclusive, paid-up, irrevocable, world-wide license to publish or reproduce the published form of this document, or allow others to do so, for U.S. Government purposes.

## Thesis Organization

This thesis follows the journal paper format discussed in the Graduate College Thesis Manual. Two papers to be submitted to peer reviewed journal appear as chapters 2 and 3 preceded by general introduction and followed by general conclusions chapters. Chapter 1 contains general introductions to the research and includes background information on the materials used and relevant recent research. Chapter 2, "Biomimetic Calcium Phosphate Precipitation on Nanoscale Pentablock Polymer Micelles," proves calcium phosphate precipitation onto the surface of self-assembling Pluronic® F127 and PDEAEM-F127-PDEAEM pentablock copolymers. Chapter 3, "Preparation of Tri-and Pentablock Polymer-Calcium Phosphate Gel Nanocomposites," examines gel formation in the presence of calcium phosphate. Ionic concentrations are varied and presence of a polymer gel-calcium phosphate nanocomposite is proved. Chapter 4, "General Conclusions," concludes this thesis. A summary of both studies is presented as well as some discussion and necessary future work.

## Abstract

In an effort to mimic the growth of natural bone, self-assembling, micelle and gel-forming copolymers were used as a template for calcium phosphate precipitation. Because of the cationic characteristics imparted by PDEAEM end group additions to commercially available Pluronic® F127, a direct ionic attraction mechanism was utilized and a polymer-brushite nanocomposite spheres were produced. Brushite coated spherical micelles with diameters of ~ 40 nm, and agglomerates of these particles (on the order of 0.5  $\mu\text{m}$ ) were obtained. Thickness and durability of the calcium phosphate coating, and the extent of agglomeration were studied. The coating has been shown to be robust enough to retain its integrity even below polymer critical micelle concentration and/or temperature. Calcium phosphate-polymer gel nanocomposites were also prepared. Gel samples appeared as a single phase network of agglomerated spherical micelles, and had a final calcium phosphate concentration of up to 15 wt%. Analysis with x-ray diffraction and NMR indicated a disordered brushite phase with the phosphate groups linking inorganic phase to the polymer.

## Chapter 1: General Introduction

Calcium phosphate ceramics, especially the tricalcium phosphate, hydroxyapatite, and brushite phases have been studied for many years. The latter two phases are of particular interest as implant material because of their good biocompatibility. Because they occur naturally in bone and dentin, they are not rejected by the body and are sometimes used as coatings for other less biocompatible materials. Many templates can be used to guide the nucleation and growth of these calcium phosphates. For example, chemically treated titanium has been coated with hydroxyapatite to improve its bone bonding ability[1, 2]. Even self assembling organic molecules can be used as substrates.

Bioinspired materials are of particular interest because of their possible implications in both artificial bone growth, and in the nano-manufacturing field. By understanding how hydroxyapatite precipitates onto self-assembling synthetic polymer micelles, we move a step closer to understanding how the similar process occurs in bone growth. At the same time, the procedure reproducibly produces spheres of calcium phosphate ceramics that could possibly be used in future nano-bio applications, like more biocompatible and bioactive implants and coatings.

In an effort to mimic the growth of natural bone, which involves precipitation of hydroxyapatite on proteins like collagen, a pentablock self assembling polymer was used as a nano-structured template. Formation of calcium phosphates on self-assembled triblock and

pentablock polymer surfaces from aqueous solutions was investigated. Characteristics and stability of the polymer/calcium phosphate hybrid materials were studied by traditional and cryo TEM, EDS, XRD, NMR, and Synchrotron small angle x-ray scattering. Experimental results indicated that calcium phosphate can be made to precipitate onto the polymer micelles.

## **1.1 Background Information**

In designing new materials, Nature gives many exciting sources of ideas and inspiration. From DNA replication to cell membranes selective transport, processes naturally occurring in biology have been studied for years and are far beyond anything that can be reproduced in a lab in their complexity and robustness. Of particular interest in the biomedical implant field are the structure and assembly mechanisms in load bearing body materials such as bone.

### ***Biological Inspiration***

In Nature, bones form first as self assembling matrices of collagen fibrils. Collagen, a tough load-bearing protein, forms bundles of triple helices which then form into larger assemblies of layers or lamellae. These layers act as the guide for hydroxyapatite precipitation[3].

Hydroxyapatite forms on the collagen surfaces and gives the bone its rigidity and shape.

This collagen self assembly is illustrated in Figure 1.

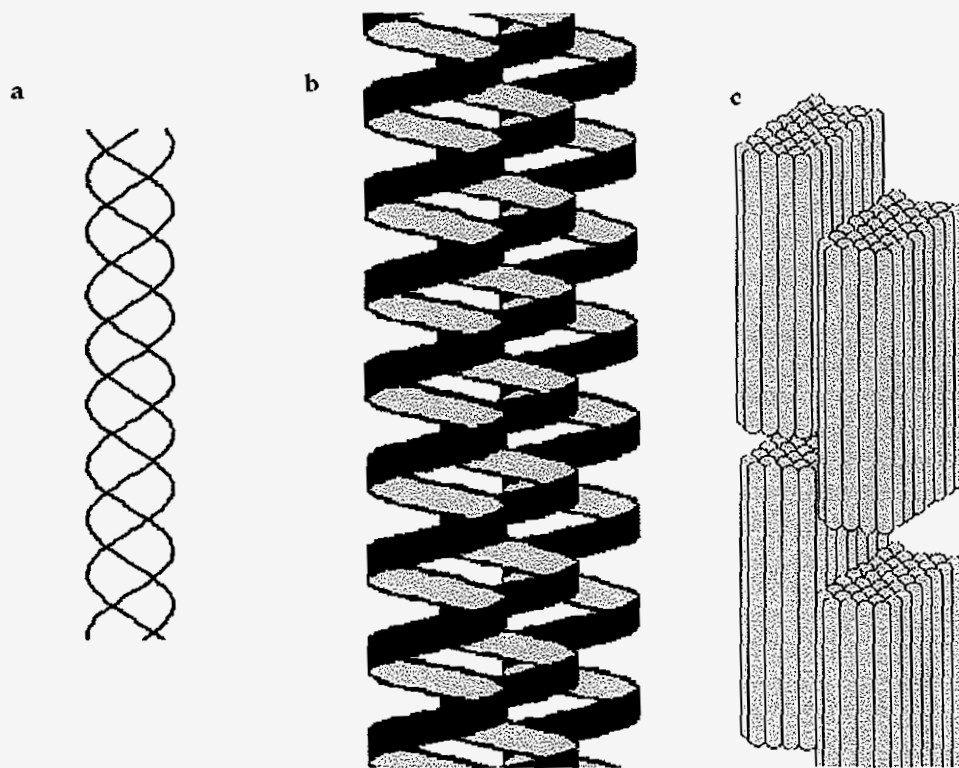


**Figure 1:** Organization of collagen framework: (a) single collagen triple helix protein, (b) bundle of collagen proteins, (c) assembly of collagen fibrils crystallization sites.

### *Calcium Phosphate*

Hydroxyapatite is a calcium phosphate ceramic with the chemical formula  $\text{Ca}_5(\text{PO}_4)_3\text{OH}$ . It is a very well known ceramic, and has been studied extensively[4-8]. Carbonated apatite is in fact the inorganic phase in bone. Carbonated apatite is very similar to Hydroxyapatite, the only difference being that  $\text{CO}_3$  ions substitute in some of the  $\text{PO}_4$  ion positions.

Hydroxyapatite has a hexagonal crystal structure which is presented in Figure 2.

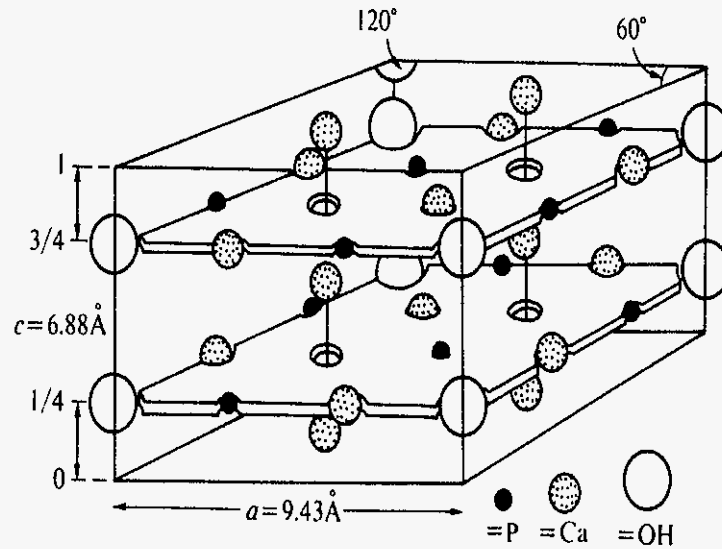


**Figure 2:** Hexagonal Hydroxyapatite Structure with  $\text{PO}_4$  shown as simply P [9].

The specific composition and structure of the calcium phosphate phase that forms is dependent on the pH of the solution. Hydroxyapatite is the most stable phase at moderate pH (from ~5 to 9). At lower pH, Brushite is the most stable. Figures 3 and 4, and Table 1 show the pH solubility diagrams of calcium and phosphate ion concentration.

**Table 1:** Common Calcium phosphate Compounds and their Formulas

Compound	Abbreviation	Formula
Brushite (Dicalcium Phosphate Dihydrate)	DCPD	$\text{CaHPO}_4 \cdot 2\text{H}_2\text{O}$
Monetite (Dicalcium Phosphate Anhydrous)	DCPA	$\text{CaHPO}_4$
Octacalcium Phosphate	OCP	$\text{Ca}_8\text{H}_2(\text{PO}_4)_6 \cdot 5\text{H}_2\text{O}$
$\alpha$ -Tricalcium Phosphate	$\alpha$ -TCP	$\alpha\text{-Ca}_3(\text{PO}_4)_2$
$\beta$ -Tricalcium Phosphate	$\beta$ -TCP	$\beta\text{-Ca}_3(\text{PO}_4)_2$
Hydroxyapatite	HAp	$\text{Ca}_{10}(\text{PO}_4)_6(\text{OH})_2$
Tetracalcium Phosphate	TTCP	$\text{Ca}_4(\text{PO}_4)_2\text{O}$

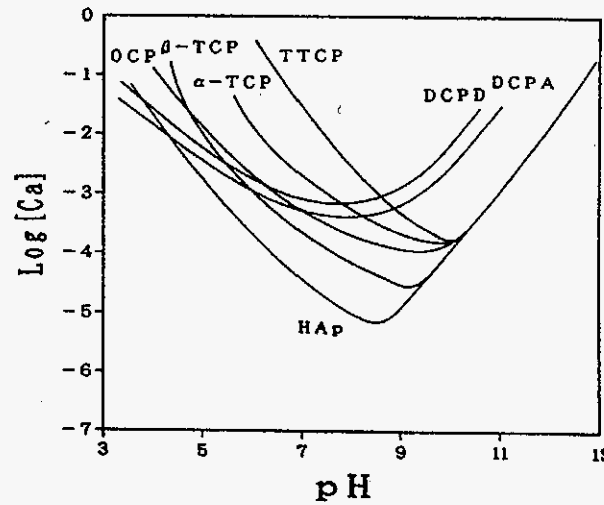


**Figure 3:** pH Solubility Diagram of Calcium Ion in the Calcium phosphate System [4].

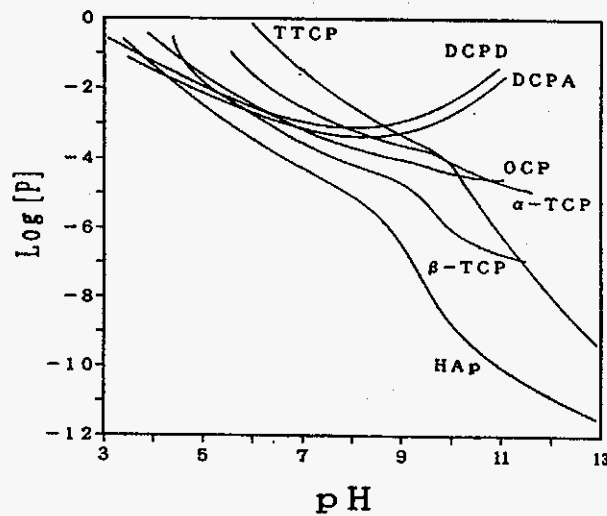


**Figure 4:** pH Solubility Diagram of Phosphate Ion in the calcium phosphate System [4].

Brushite (DCPD) is also a common calcium phosphate ceramic used in the biomedical field. Its chemical formula is  $\text{CaPO}_3(\text{OH}) \cdot 2\text{H}_2\text{O}$ . Brushite crystallizes into a non-centrosymmetric structure in the space group Ia [10]. Figure 5 shows the structure of Brushite. It has good biocompatibility and is actually desirable over Hydroxyapatite when making products like bone cements[6].

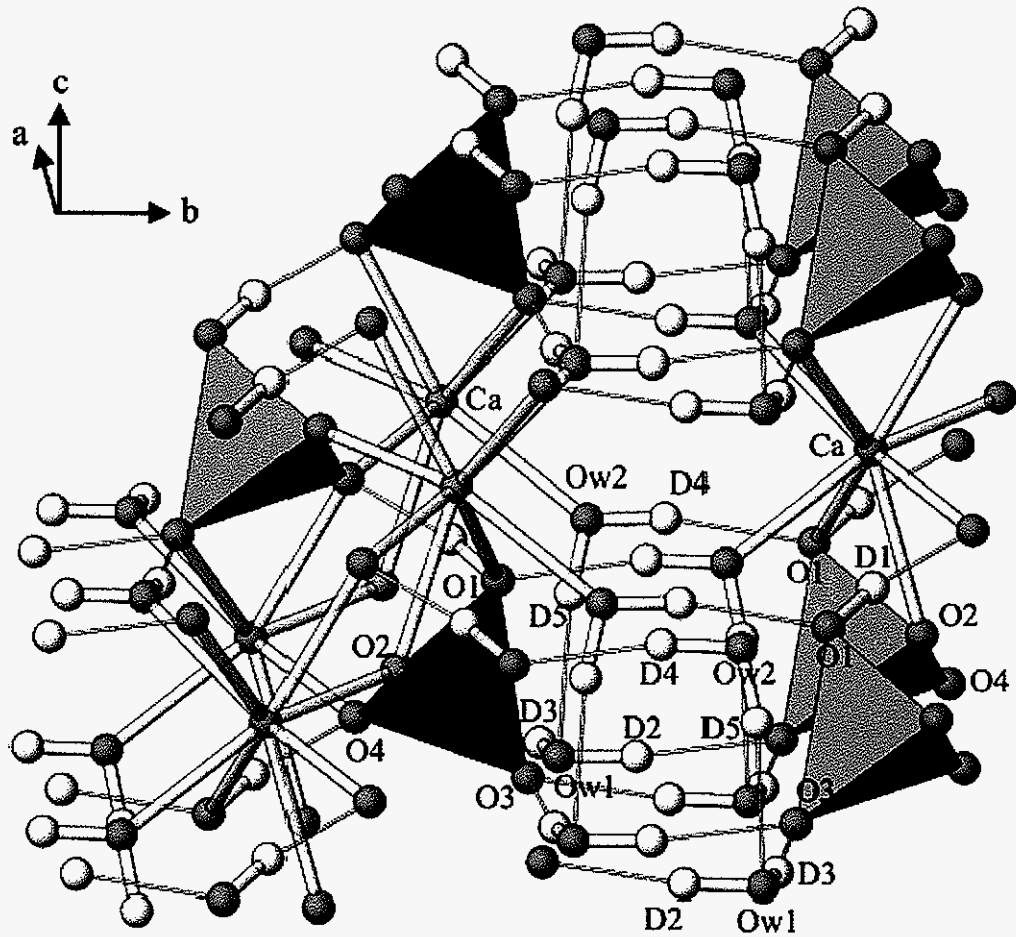
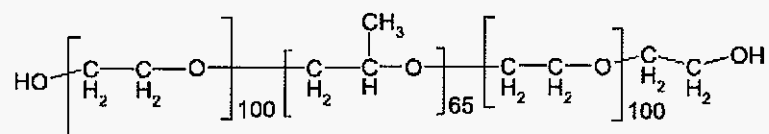


**Figure 5:** Brushite Crystal Structure. The Hydrogen (D), Calcium (Ca), and Oxygen (O) atoms are labeled and the  $\text{PO}_4$  Ions are shown as solid tetrahedral [10].

Because they occur naturally in the body, Hydroxyapatite, Brushite, and other calcium phosphates make excellent implant materials. The body is compatible with these compounds and responds with little or no foreign body response. For this reason, other materials are sometimes coated with hydroxyapatite to improve their biocompatibility or bone bonding ability.

### *Synthetic Self-Assembling Block copolymers as Templates*

In order to mimic Nature's use of self assembling macromolecular collagen proteins, synthetic polymers are used. Specifically, a pH sensitive micelle and gel forming modified Pluronic F127 polymer is used in this study. As illustrated below, Pluronic F127 is a triblock copolymer of poly(ethylene oxide)/poly(propylene oxide)/poly(ethylene oxide) [11].



For this study, the Pluronic F127 polymer has been modified with poly(2-diethylaminoethyl methacrylate), PDEAEM, end groups replacing the -OH to obtain a pH sensitive self assembling pentablock polymer. Because of the polymer's hydrophobic poly(propylene oxide) middle and its hydrophilic poly(ethylene oxide) and PDEAEM end groups, it folds and self assembles into micelles when dissolved at low concentration in water at room temperature. Furthermore, this pentablock polymer also forms a thick gel at room temperature and at polymer concentrations above 10 wt%. The polymer is completely soluble at temperatures below 10°C, but when heated above that, the solution congeals into a viscous gel [11-16]. A phase diagram of the modified pentablock polymer is presented in Figure 6, and a cryo-TEM image of micelles in solution are presented in Figure 7.

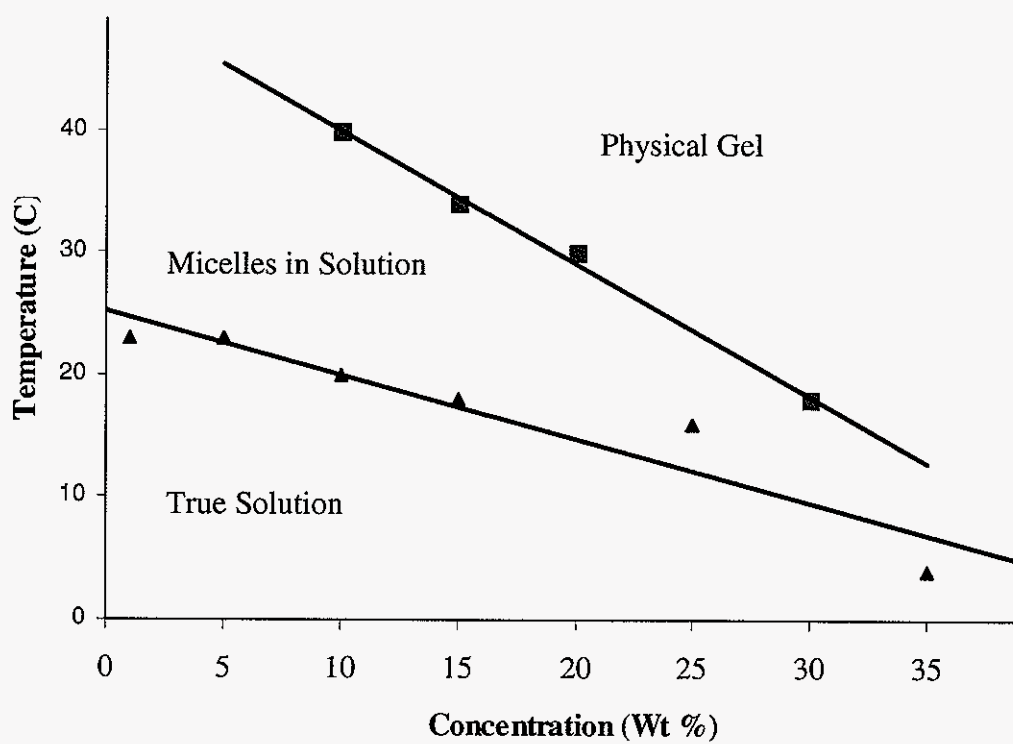


**Figure 6:** Phase Transitions of Modified Pentablock Polymer at pH 7

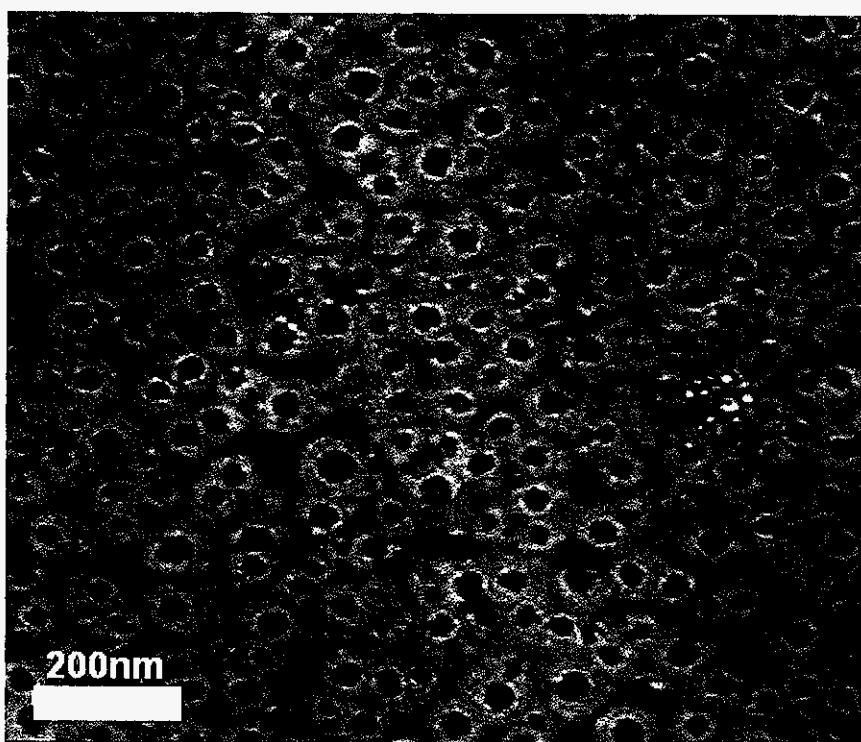


**Figure 7:** Cryo-TEM Image of Pluronic Polymer Micelle [11]

### *Organic-Inorganic Nanocomposite Materials*

By floating a thin film of stearic acid solution in chloroform over a saturated aqueous solution of calcium phosphate, it is possible to form continuous films of apatite [17, 18]. Because of its hydrophobic hydrocarbon chain, when floating on water, stearic acid aligns itself with its negatively charged end just below the surface of the water. Positively charged  $\text{Ca}^{2+}$  ions in the aqueous solution are attracted to the carboxylic acid groups. Once the carboxylate groups are covered with  $\text{Ca}^{2+}$ , it serves as a growth site for calcium phosphate by accumulating  $\text{Ca}^{2+}$  and  $\text{PO}_4^{3-}$  ions. The ions continue to attach to the surface of the film and form a continuous ceramic coating. The coating is initially amorphous, but after sintering at  $900\text{ }^\circ\text{C}$  for 2 hours, it is crystalline. A schematic of the above process is given in Figure 8. In this case, Xu et al used a solution of supersaturated  $\text{Ca}(\text{HCO}_3)_2$ , and  $\text{Na}_3\text{PO}_4$  [17]. This was done in an effort to produce Carbonate Apatite ( $\text{Ca}_5(\text{PO}_4)_{3-x}(\text{OH})_1(\text{CO}_3)_x$ ). Carbonate Apatite (CAp) is very similar to Hydroxyapatite as the only difference is that some of the  $\text{PO}_4$  ions are replaced with  $\text{CO}_3$ .

Similar techniques have been applied to solid polymer systems. For example, pHEMA strips have been coated with hydroxyapatite [19, 20]. In this experiment, Song et al used the carboxylate groups on the surface of the hydrogel as nucleation sites for calcium phosphate. At temperatures above  $95^\circ\text{C}$ , and with aging times of over 10 hours, a surface layer of calcium and phosphorous was detected with EDS, and small  $\sim 10\text{ }\mu\text{m}$  diameter hydroxyapatite spherical clusters were confirmed with XRD SEM.

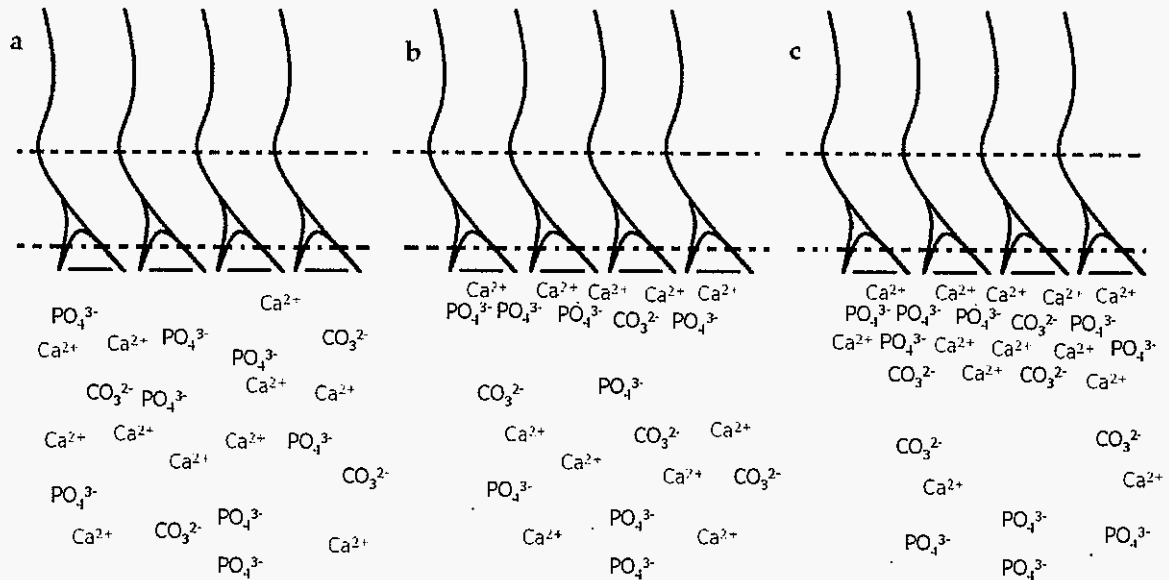


**Figure 8:** Schematic of carbonate apatite thin film growth. a) initial stearic acid thin film floating on calcium phosphate solution. b) calcium and phosphate nucleation. c) growth of continuous CAP thin film

In another study, chemically activated cellulose fibers were used as a template for calcium phosphate. Muller et al were able to produce 30  $\mu\text{m}$  thick homogeneous coatings of octacalcium phosphate and hydroxyl carbonated apatite [21]. This was achieved by treating the cellulose fibers treated with a  $\text{Ca}(\text{OH})_2$  and then soaking in simulated body fluid for 21 days. In this case, Muller et al propose that it is the cellulose hydroxyl groups exposed to  $\text{Ca}(\text{OH})_2$  that trigger calcium phosphate nucleation.

Even aqueous polymers have been used as templates for calcium phosphate nucleation. Rusu et al used the biopolymer chitosan as the template for their organic-inorganic nanocomposite [22]. After mixing chitosan, calcium chloride, and ammonium dihydrogen phosphate,

Brushite nanoparticles were formed. The pH of the solution was raised to 10 and the Brushite converted to hydroxyapatite over a period of 24 hours. Rusu et al proposed that as pH increases, the chitosan polymers extend into a random coil conformation forming a random polymer network.

### References

1. Jonasova, L., et al., *Biomimetic apatite formation on chemically treated titanium*. Biomaterials, 2004. **25**(7-8): p. 1187-1194.
2. Jonasova, L., et al., *Hydroxyapatite formation on alkali-treated titanium with different content of Na<sup>+</sup> in the surface layer*. Biomaterials, 2002. **23**(15): p. 3095-3101.
3. Rao, P.R., *Biomimetics*. Sadhana, 2003. **28**(3&4): p. 657-676.
4. Oonishi, H. and K. Oomamiuda, eds. *Degradation/resorption in bioactive ceramics in orthopaedics*. First ed. Handbook of Biomaterial Properties, ed. J. Black and G. Hastings. 1998, Chapman and Hall: London. 590.
5. Fulmer, M.T., et al., *Measurements of the solubilities and dissolution rates of several hydroxyapatites*. Biomaterials, 2002. **23**(3): p. 751-755.
6. Malsy, A. and M. Bohner, *Brushite conversion into apatite*. European Cells and Materials, 2005. **10**(Suppl. 1): p. 28.
7. Ito, A., et al., *Solubility product of OH-carbonated hydroxyapatite*. Journal of Biomedical Materials Research, 1997. **36**(4): p. 522-528.
8. Brown, W.E. and L.C. Chow, *Thermodynamics of apatite crystal growth and dissolution*. Journal of Crystal Growth, 1981. **53**(1): p. 31-41.
9. Elliott, J.C., *Structure and Chemistry of the Apatites and other Calcium Orthophosphates*. Studies in inorganic chemistry. Vol. 18. 1994, Amsterdam: Elsevier. 389.
10. Schofield, P.F., et al., *The role of hydrogen bonding in the thermal expansion and dehydration of brushite, di-calcium phosphate dihydrate*. Physics and Chemistry of Minerals, 2004. **31**(9): p. 606-624.
11. Determan, M.D., et al., *Synthesis and characterization of temperature and pH-responsive pentablock copolymers*. Polymer, 2005. **46**(18): p. 6933-6946.
12. Anderson, B.C., et al., *Synthesis and Characterization of Diblock and Gel-Forming Pentablock Copolymers of Tertiary Amine Methacrylates, Poly(ethylene glycol), and Poly(propylene glycol)*. Macromolecules, 2003. **36**(5): p. 1670-1676.
13. Anderson, B.C., et al., *The effect of salts on the micellization temperature of aqueous poly(ethylene oxide)-*b*-poly(propylene oxide)-*b*-poly(ethylene*

- oxide) solutions and the dissolution rate and water diffusion coefficient in their corresponding gels.* Journal of Pharmaceutical Sciences, 2002. **91**(1): p. 180-188.
14. Anderson, B.C., N.K. Pandit, and S.K. Mallapragada, *Understanding drug release from poly(ethylene oxide)-b-poly(propylene oxide)-b-poly(ethylene oxide) gels.* Journal of Controlled Release, 2001. **70**(1-2): p. 157-167.
  15. Anderson, B.C. and S.K. Mallapragada, *Synthesis and characterization of injectable, water-soluble copolymers of tertiary amine methacrylates and poly(ethylene glycol) containing methacrylates.* Biomaterials, 2002. **23**(22): p. 4345-4352.
  16. Ivanova, R., B. Lindman, and P. Alexandridis, *Evolution in structural polymorphism of Pluronic F127 poly(ethylene oxide)-poly(propylene oxide) block copolymer in ternary systems with water and pharmaceutically acceptable organic solvents: From 'glycols' to 'oils'.* Langmuir, 2000. **16**(23): p. 9058-9069.
  17. Xu, G., I.A. Aksay, and J.T. Groves, *Continuous crystalline carbonate apatite thin films. A biomimetic approach.* Journal of the American Chemical Society, 2001. **123**(10): p. 2196-2203.
  18. Xu, G., et al., *Biomimetic synthesis of macroscopic-scale calcium carbonate thin films. Evidence for a multistep assembly process.* Journal of the American Chemical Society, 1998. **120**(46): p. 11977-11985.
  19. Song, J., E. Saiz, and C.R. Bertozzi, *A new approach to mineralization of biocompatible hydrogel scaffolds: An efficient process toward 3-dimensional bonelike composites.* Journal of the American Chemical Society, 2003. **125**(5): p. 1236-1243.
  20. Song, J., E. Saiz, and C.R. Bertozzi, *Preparation of pHEMA-CP composites with high interfacial adhesion via template-driven mineralization.* Journal of the European Ceramic Society, 2003. **23**(15): p. 2905-2919.
  21. Muller, F.A., et al. *Biomimetic Apatite Formation on Chemically Modified Cellulose Templates.* in *The Annual Meeting of the International Society for Ceramics in Medicine, Nov 6-9 2003.* 2004. Porto, Portugal: Trans Tech Publications Ltd.
  22. Rusu, V.M., et al., *Size-controlled hydroxyapatite nanoparticles as self-organized organic-inorganic composite materials.* Biomaterials, 2005. **26**(26): p. 5414-5426.

## **Chapter 2: Biomimetic Calcium Phosphate Precipitation on Nanoscale Pentablock Polymer Micelles**

D. Enlow\*, T. Pepper\*\*, M. Determan\*\*\*, S. Mallapragada\*\*\*, and M. Akinc\*

\* Materials Science and Engineering and Ames Laboratory \*\* Bessey Microscopy Facility

\*\*\* Department of Chemical Engineering and Ames Laboratory, Iowa State University,  
Ames Iowa.

### **Abstract**

In an effort to mimic the growth of natural bone, a modified Pluronic F127 pentablock micelle-forming polymer was used as a template for calcium phosphate precipitation. Because of the cationic characteristics imparted by the PDEAEM polymer end groups, a direct ionic attraction mechanism was utilized and a polymer-brushite nanocomposite spheres were produced. Consistent with similar experiments in literature [1, 2], spherical particles with diameters of ~ 40 nm, and agglomerates of these particles (on the order of 0.5  $\mu\text{m}$ ) were obtained. Experimental conditions such as calcium and phosphate concentrations and aging time were varied to control the size of the calcium phosphate coating, and the extent of agglomeration. The coating has been shown to be robust enough to retain its integrity even below polymer critical micelle concentration and/or temperature.

### *Introduction*

Because of their excellent biocompatibility, calcium phosphate compounds for in vitro applications have been studied extensively. For example, biomimetic apatite coatings for titanium has been studied [3, 4]. Because apatite is a natural component in bone, this coating can improve the implants bone bonding and its biocompatibility. Other than large-sized implant materials, polymer scaffolds can be used substrates and coated with calcium phosphate.

Song et al used poly(2-hydroxyethyl methacrylate), (pHEMA) scaffolds as a template to drive mineralization [5, 6]. In this study, hydroxyapatite was dissolved in water with the addition of hydrochloric acid. Urea was then added and finally, pHEMA hydrogel strips were immersed into this solution. This solution was then heated at 0.6°C/min to 95°C. After washing and drying the strips, strong phosphorous and calcium EDS signals were detected on the surfaces. These samples, however, appear amorphous based on XRD patterns. By decreasing the heating rate to less than 0.2°C/min, or extending mineralization time by 10 hours after reaching 95°C, additional precipitation occurred on the hydrogel surface. This precipitation occurred clustered into spheres and showed some of the characteristic hydroxyapatite x-ray diffraction peaks.

Song et al proposed that the combination of urea driven homogenous precipitation and the lower interfacial energy available on the hydrogel surface drove precipitation. Thermal decomposition of the urea forced the solution's pH to increase and the decrease of calcium phosphate solubility with pH to facilitate homogeneous precipitation. The carboxylate rich

pHEMA surface then provided nucleation sites for precipitation and growth of the calcium phosphate layer.

Simple organic molecules can be used as substrates for calcium phosphate precipitation. Xu et al demonstrated that it was possible to use a stearic acid film to guide calcium phosphate precipitation and produce a continuous thin film of apatite [7]. By floating a thin film of stearic acid solution in chloroform on a calcium phosphate solution, they showed that it was possible to form continuous films of apatite. With its hydrophobic hydrocarbon chain, stearic acid aligns itself with its negatively charged end just below the surface of the water. Positively charged  $\text{Ca}^{2+}$  ions are attracted to the acid surface, and negatively charged  $\text{PO}_4^{3-}$  ions follow. The ions continue to attach to the surface of the film until equilibrium is reached and a continuous ceramic coating is formed. Initially amorphous, after sintering at  $900^\circ\text{C}$  for 2 hours, crystalline carbonated apatite is observed. Xu et al propose direct attraction of the  $\text{Ca}^{2+}$  ions to the negatively charged stearic acid surface, and showed that overall shape as well morphology can be maintained even with radical environmental changes like drying and heat treatment.

It is also possible to take this process a step further. More complex organic molecules can also be used to guide calcium phosphate precipitation. Zhao and Ma demonstrated a procedure in which mesoporous hydroxyapatite was synthesized on the surface of Pluronic® F127 polymer micelles [1].

Pluronic® F127 is an ABA type copolymer of poly(ethylene oxide), poly(propylene oxide), and poly(ethylene oxide). In aqueous solutions, the PEO end chains are hydrophilic while the PPO middle chain is hydrophobic. This causes the polymer to self assemble into micelles when dissolved at a high enough concentration. Zhao and Ma proposed an inorganic precursor model to explain hydroxyapatite precipitation onto the surface of the micelles.

By supplying calcium in the form of calcium D-pantothenane monohydrate, Zhao and Ma proposed a mechanism with the polymer micelle surfactant being associated with hydrogen bonding to the calcium D-pantothenane monohydrate inorganic precursor. Phosphate ions were supplied in the form of potassium hydrogenphosphate trihydrate that were then attracted to the nucleation sites formed in the above sites. The solution was gradually titrated with potassium hydrogen phosphate trihydrate and with ammonia to reach a final pH of 12 and a calcium to phosphate ion ratio of 1.667:1. After separation and sintering, the authors presented TEM micrographs showing hydroxyapatite particles with a porous interior structure. Zhao and Ma's proposed possible explanation for this is illustrated in Figure 1.

After the thin inorganic precursor layer formed around the Pluronic® F127 micelle and titration with phosphate and ammonia was started, hydroxyapatite began precipitating on the micelle surface. The calcium phosphate coated micelles grew until they eventually agglomerate. With increasing concentration of phosphate, hydroxyapatite continued to precipitate on the surface of the agglomerated mesoparticle. During calcination, the organic polymer micelle template burned out and leaving the porous structure observed.

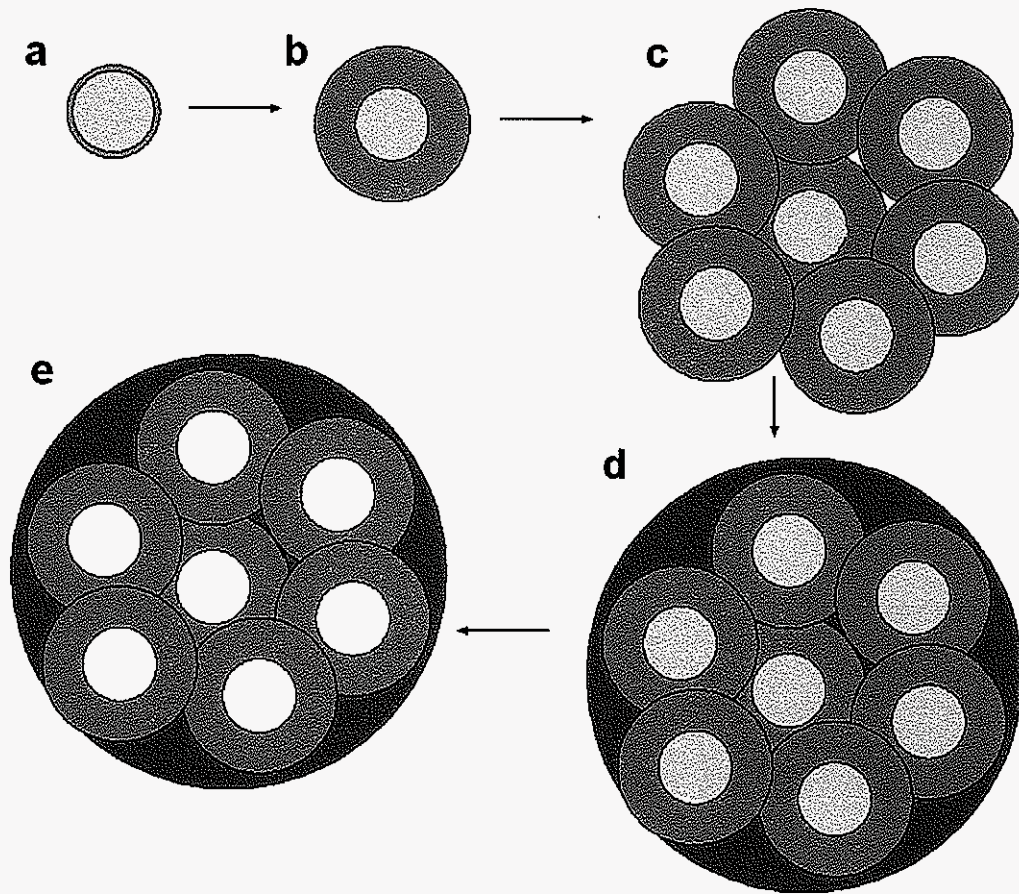


**Figure 1:** Formation of mesoporous spherical hydroxyapatite Powders. a) Spherical micelle with inorganic precursor and  $\text{Ca}^{2+}$  monolayer b) Hydroxyapatite coated micelle c) Aggregated cluster of hydroxyapatite coated micelles d) Spherical aggregate e) After calcination, spherical mesoporous hydroxyapatite particle.

By combining aspects of several of these experiments, a more direct and effective precipitation method may be possible. The pentablock polymer developed by Determan et al [8] is a more environmentally sensitive modification of the same Pluronic® F127 used by Zhao and Ma. Like Pluronic® F127, the pentablock polymer self assembles into micelles when in solution at low concentration, but, because of the poly(2-diethylaminoethyl

methacrylate), PDEAEM, end groups on either side of the Pluronic® F127 chain, the polymer is pH sensitive and has cationic characteristics at low pH.

Similar to the Xu et al thin film experiment, the cationic characteristics of the PDEAEM allows direct ionic attraction to the polymer surface. Built on the Pluronic® F127 backbone, the pentablock copolymer forms micelles with very similar size and shape to those in the Zhao and Ma experiment. Finally, like Song et al, the additional functional groups on the micelle surface should provide many low interfacial energy nucleation sites for precipitation of calcium phosphate. Even without the inorganic precursor molecules used by Zhao and Ma, direct precipitation on the Pluronic® F127 should be possible. Pluronic® F127 micelles have polar OH end groups that when assembled as a surface provide slightly negatively charged sites for nucleation.

### ***Materials and Methods***

Unless otherwise noted, all chemicals in this study were obtained from Fisher Scientific and are of laboratory grade and purity. Precipitation of calcium phosphate onto the polymer micelles was achieved using solutions of calcium nitrate ( $\text{Ca}(\text{NO}_3)_2$ ) and either ammonium dihydrogen phosphate ( $\text{NH}_4\text{H}_2\text{PO}_4$ ) or phosphoric acid ( $\text{H}_3\text{PO}_4$ ), as well as either the PDEAEM<sub>35</sub>-F127-PDEAEM<sub>35</sub> modified pentablock polymer or the commercially available Pluronic® F127 polymer. A dilute solution of calcium phosphate was prepared by mixing 0.5M solutions of ammonium dihydrogen phosphate and calcium nitrate. In an effort to obtain the 1.667 Ca:P ratio found in hydroxyapatite, these two solutions were mixed at a ratio of 120ml ammonium dihydrogen phosphate to 200ml calcium nitrate. This solution was then

stirred for 30 minutes until a white precipitate formed. The mixture was then centrifuged and the clear supernatant was drawn off as the saturated calcium phosphate solution. This supernatant solution had a pH of 2.95. The precipitate was rinsed and dried in a desiccator.

10 ml of this calcium phosphate solution was mixed with an equal amount of 1.0wt% polymer solution yielding a solution of 0.5wt% polymer, and half of the saturated calcium phosphate ion concentrations. This solution was placed in a 25° C temperature controlled water bath, and allowed to age. The samples were taken after 30min, 1hr, 24r, and after 2 weeks and imaged using a transmission electron microscope. Micrographs taken of the 24hr and the 2 week samples were indistinguishable, implying that the system reaches equilibrium within the first 24 hours.

The polymer / calcium phosphate solution was separated from coated micelles by dialysis for characterization. The dialysis was accomplished using 14000 molecular weight pore dialysis tubing. 10cm of dialysis tubing was cut and soaked in de-ionized water. One end of the tubing was clamped with dialysis clips and 20 mL of the mixed polymer-inorganic solution was added. The other end of the tubing was also clipped leaving 2 cm space on top. The dialysis pouch was placed in 4 liters of de-ionized water and stirred for at least 8 hours. The water bath was replaced with de-ionized water twice a day for a total of 5 times and finally, the purified ceramic coated micelle solution was collected and vacuum dried for analysis with EDS.

A higher ionic concentration solution was prepared by mixing 4.0M solutions of phosphoric acid and calcium nitrate. Sodium hydroxide was added until the solution reached a pH of 1.0 and a cloudy precipitate formed. Like the dilute solution described above, this solution was stirred for 30 min and then centrifuged. The resulting supernatant was mixed with an equal amount of 1.0wt% polymer solution yielding a solution of 0.5wt% polymer, and half of the inorganic ion concentration. These samples were prepared for TEM after aging for 30 min and 60 hr.

### *Characterization*

To prepare the TEM samples, 50 $\mu$ L of the aqueous sample was placed onto a formvar coated copper grid for 1 minute allowing contents to settle. Most of the supernatant was wicked away and 1% phosphotungstic acid (pH 6.2) was applied for 30 seconds as a negative contrast stain. The grid was wicked and allowed to dry. Images were captured on a JEOL 1200EX II scanning transmission electron microscope (Japan Electron Optic Laboratories, Peabody, MA) using a Megaview III digital camera and SIS Pro. Software (Soft Imaging Systems Inc., LLC, Lakewood, CO).

Qualitative chemical constituents of the samples were determined by energy dispersive spectroscopy (EDS) attached to a JEOL 6060 LV-SEM (Oxford Instruments). The electron beam was set at an accelerating voltage of 20kV and the chemical x-ray spectrum was analyzed against the INCA software internal standards. X-ray powder diffraction patterns of samples were obtained using a Scintag XGEN-400 theta-theta x-ray diffractometer. The Cu K $\alpha$  x-ray source was set to 45kV and 40mA, and the scanning rate was 1 $^\circ$ /min over a range

of  $10^\circ - 70^\circ$ . Phase analysis was done using the ICDD database and the Scintag DMSNT search / match software.

Small angle X-ray scattering Synchrotron experiments were conducted at Argonne National Lab. Aqueous pH 2.95 Pluronic® F127 micelle samples were transferred to 1.3 mm OD quartz capillary tubes with 0.1 mm nominal wall thickness and sealed to prevent evaporation. SAXS measurements were carried out on the instrument at the 12-ID beam line at the Advanced Photon Source. The experiments were conducted at three different temperatures;  $5^\circ\text{C}$ ,  $25^\circ\text{C}$ , and  $40^\circ\text{C}$ . The  $5^\circ\text{C}$  sample was below the critical micellation temperature of the polymer. Guinier regression was used to calculate average particle size at each temperature [9].

### ***Results and Discussion***

The precipitate formed upon initial mixing of the 0.5M  $\text{Ca}(\text{NO}_3)_2$  and  $\text{NH}_4\text{H}_2\text{PO}_4$  aqueous solutions showed a mixture of Brushite (dicalcium phosphate dihydrate,  $\text{CaPO}_3(\text{OH}) \cdot 2\text{H}_2\text{O}$ ) and Monetite (dicalcium phosphate anhydrous,  $\text{CaPO}_3(\text{OH})$ ). The x-ray diffraction patterns are presented in Figure 2. The figure highlights both the Brushite peaks and the Monetite peaks.

This is consistent with the phases predicted by the calcium phosphate pH-concentration equilibrium diagram, as well as with what Rusu et al observed after mixing calcium chloride and ammonium dihydrogen phosphate [2].

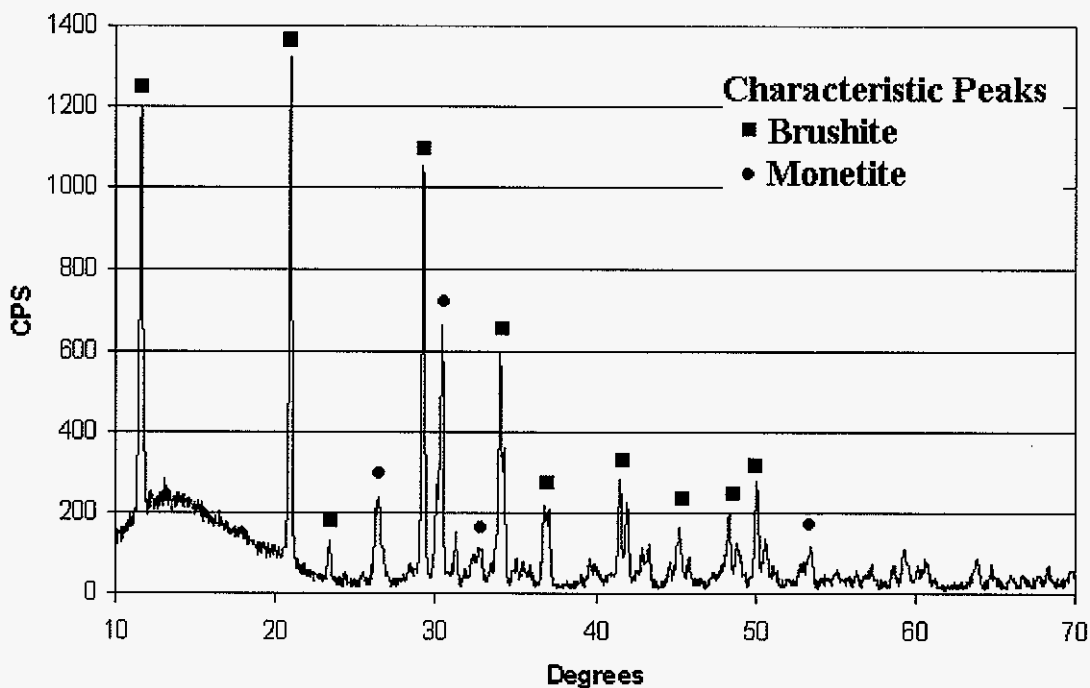


**Figure 2:** Phase Identification of Calcium Phosphate Precipitate

After dialysis all the calcium and phosphate ions and all the non-coated micelles were removed from the suspension. Only micelles that were coated by calcium phosphate were left in the solution. These samples indicated, strong calcium and phosphorous signals in the EDS Spectrum. Along with this qualitative evidence, quantitative analysis showed the calcium to phosphorus ratio close to unity as one would expect from Brushite and Monetite.

After confirming that calcium phosphate, in this case a mixture of brushite and monetite, formed, morphology of the coated micelles was studied by TEM. Figure 4 is a negative-stain TEM image of the pentablock polymer dissolved at 0.5 wt% in deionized water. The 20 – 40 nm diameter spheres seen when imaged with this technique compare very well to the 12- 25

nm pentablock copolymer micelle core radius seen in the cryo-TEM image presented by Determan et al [8].

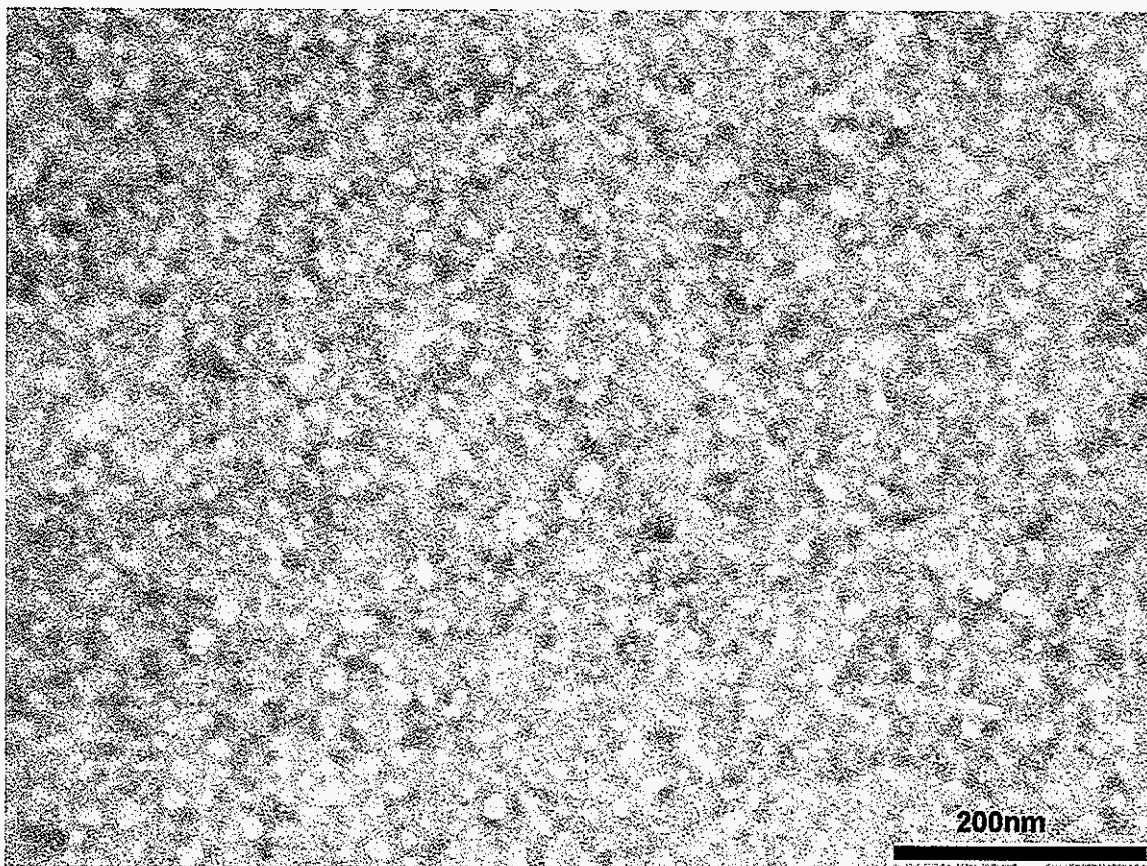


**Figure 4:** Traditional, Negative-Stained micrograph of Pentablock Polymer Micelles

Consistent with what Zhao and Ma [1] proposed, the addition of calcium and phosphate ions to the polymer solution induces nucleation and growth of calcium phosphate onto the micelle surface. At low ionic concentration, using the pH 2.95 calcium phosphate solution, this growth occurred slowly over a period several hours. Figure 5 shows the progression of the growth process.

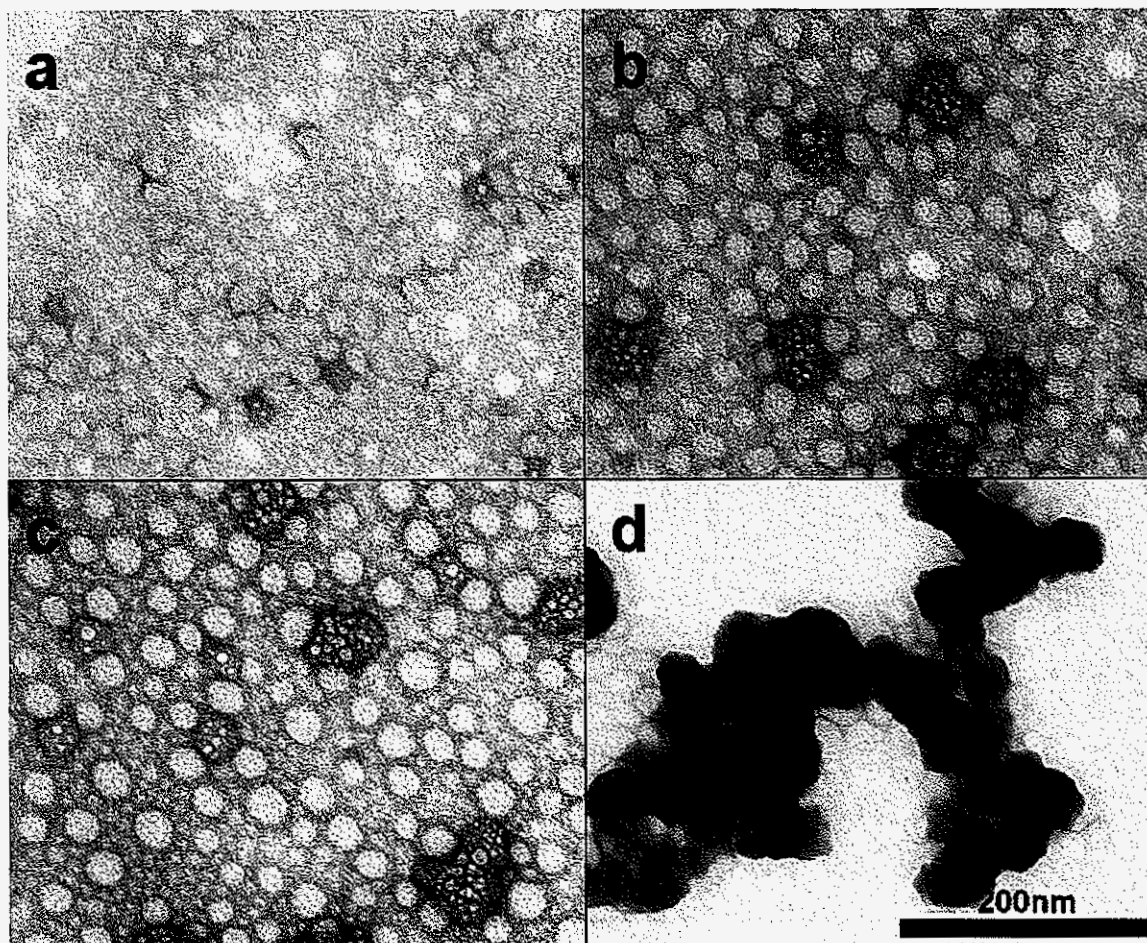


**Figure 5:** Precipitation of calcium phosphate solid phase over pentablock polymer micelles as a function of time at pH = 2.95. a) 30 min b) 1hr c) 24 hours d) 24 hours agglomerated

It was found that relatively few of the micelles were actually coated with the calcium phosphate. As seen in figure 5a, as early as 30 minutes some of the micelles begin to guide precipitation of the darker appearing more electron dense brushite / monetite coating. This ceramic coating gets more substantial and thick with time, growing to a diameter of about 40 nm, as shown in Figure 5b. However, many uncoated micelles still remain in solution.

After several hours, more calcium phosphate accumulated over micelles and they began to agglomerate into larger particles on the order of 0.5  $\mu\text{m}$  in diameter. Figures 5c and d show two different areas of the same sample after 24 hours. Figure 5c looks very similar to samples at shorter times. Like the previous samples these micelles had thin coatings and were mostly well dispersed. Figure 5d, however, shows an area of the sample where the calcium phosphate coated micelles have agglomerated. Calcium phosphate have continued to precipitate onto the agglomerated surfaces and have created a larger precipitate.

Samples prepared with the higher calcium and phosphate concentration at pH 1.0 did not display this time dependent precipitation. Apparently, the much higher ionic concentration resulted in almost instant precipitation of calcium phosphate. Figure 6 shows formation of calcium phosphate precipitation in the 0.5 weight percent pentablock polymer dissolved in the saturated solution at pH = 1.0. The sample in Figure 6a shows the solid phase formation after 30 min and Figure 6b after 50 hours. Both the 30 minute and the 50 hour samples showed precipitation and agglomeration of large brushite / monetite phases, other than the amount of calcium and phosphate formed, the two samples are practically indistinguishable.

The SAXS analysis of the pH 2.95 Pluronic® F127 samples proved calcium phosphate coating over micelles. Radius of gyration,  $R_g$ , below the critical micellization temperature (CMT) measured before aging the polymer in the calcium phosphate solution was approximately one-half of that measured above the CMT. However, for the micelles coated with calcium phosphate, the radius of gyration,  $R_g$ , was more or less constant irrespective of the temperature. These results as shown in Table 1 lead to the conclusion that, like the strong

adhesion reported by Song et al [5, 6], the calcium phosphate coating imparts some stability to the micelles, and that the coating protects the micelles from dissociating back into polymer chains which was the case for uncoated polymer micelles.

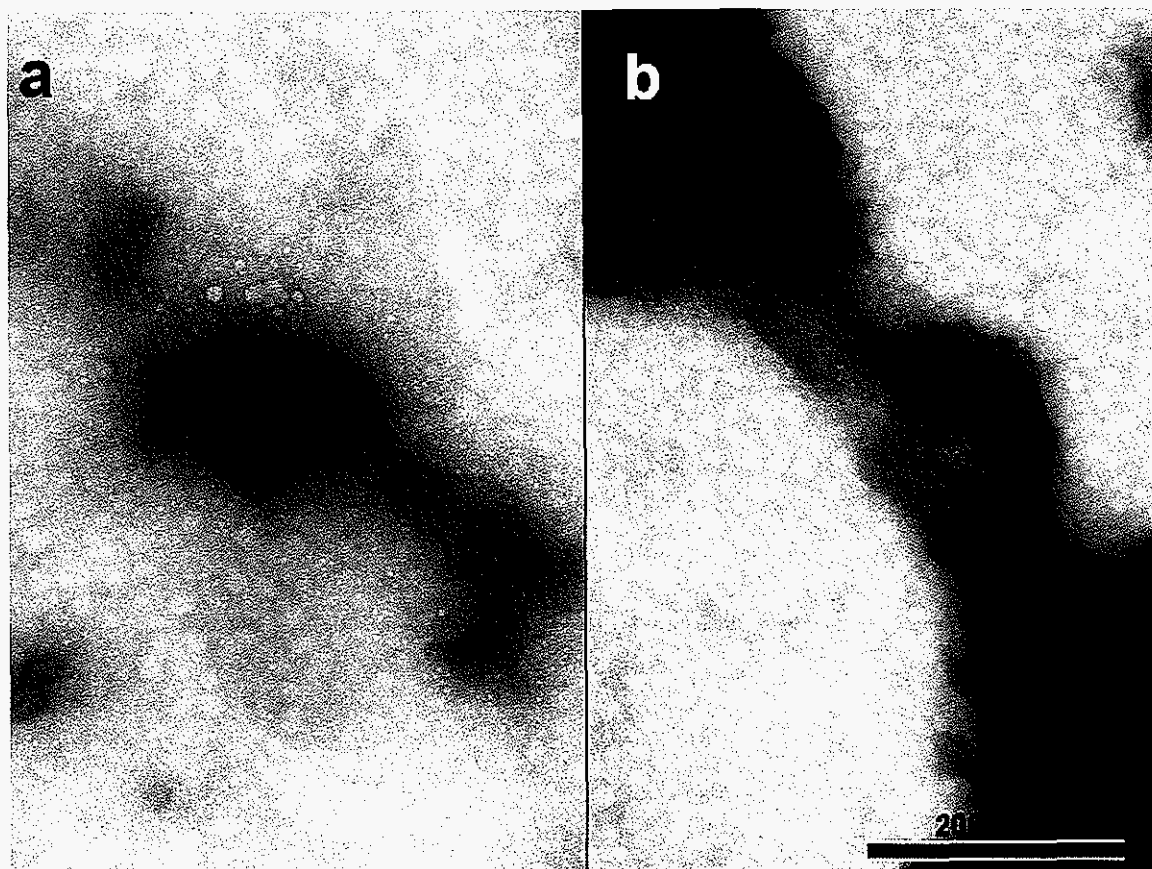


**Figure 6:** Precipitation of calcium phosphate solid phase over pentablock polymer micelles as a function of time at pH = 1.0. a) 30 min b) 50 hours

**Table 1:** Guinier Analysis of Pluronic Solution Synchrotron Data

Solvent	Temperature (°C)	$R_g$ (Å)
De-Ionized Water	5	28.2 $\pm$ 0.30
De-Ionized Water	25	50.0 $\pm$ 0.23
De-Ionized Water	40	43.9 $\pm$ 0.20
Saturated Ca P Solution	5	49.9 $\pm$ 0.09
Saturated Ca P Solution	25	52.1 $\pm$ 0.08
Saturated Ca P Solution	40	43.0 $\pm$ 0.26

This observation was further supported with the TEM analysis of the sample after dialysis. TEM shows that after several dialysis dilutions with the saturated calcium phosphate solution (no polymer in solution), the non-coated micelles were all but dialyzed out of the sample solution. The calcium phosphate-coated micelles however were still present as they did not dissolve and were too large to diffuse out of the 12-14000 MWCO dialysis tubing. Figure 7 shows two regions of the dialysis sample. Figure 7a shows a region of agglomerated calcium phosphate-coated micelles while Figure 7b shows a region that shows few disperse particles. Neither show any of the uncoated micelles that were present before dialysis (see Figures 4 and 5).

### *Conclusion*

A biomimetic process for precipitating calcium phosphate onto the surface of nano-sized polymer micelles has been developed. The resulting spherical particles have diameters of ~40 nm and agglomerates into larger particles on the order of 0.5  $\mu\text{m}$ . These spheres are composed of a brushite and monetite coating around a polymer core. Nucleation and growth of the calcium phosphate over micelles as shown by negative stained TEM images, stability of the coated micelles below critical micelle concentration and critical micellization temperature, and phase identification with EDS and x-ray diffraction, confirms that both Pluronic® F127, and the PDEAEM-F127-PDEAEM pentablock polymer micelles provide good substrates to guide the precipitation of calcium phosphate.

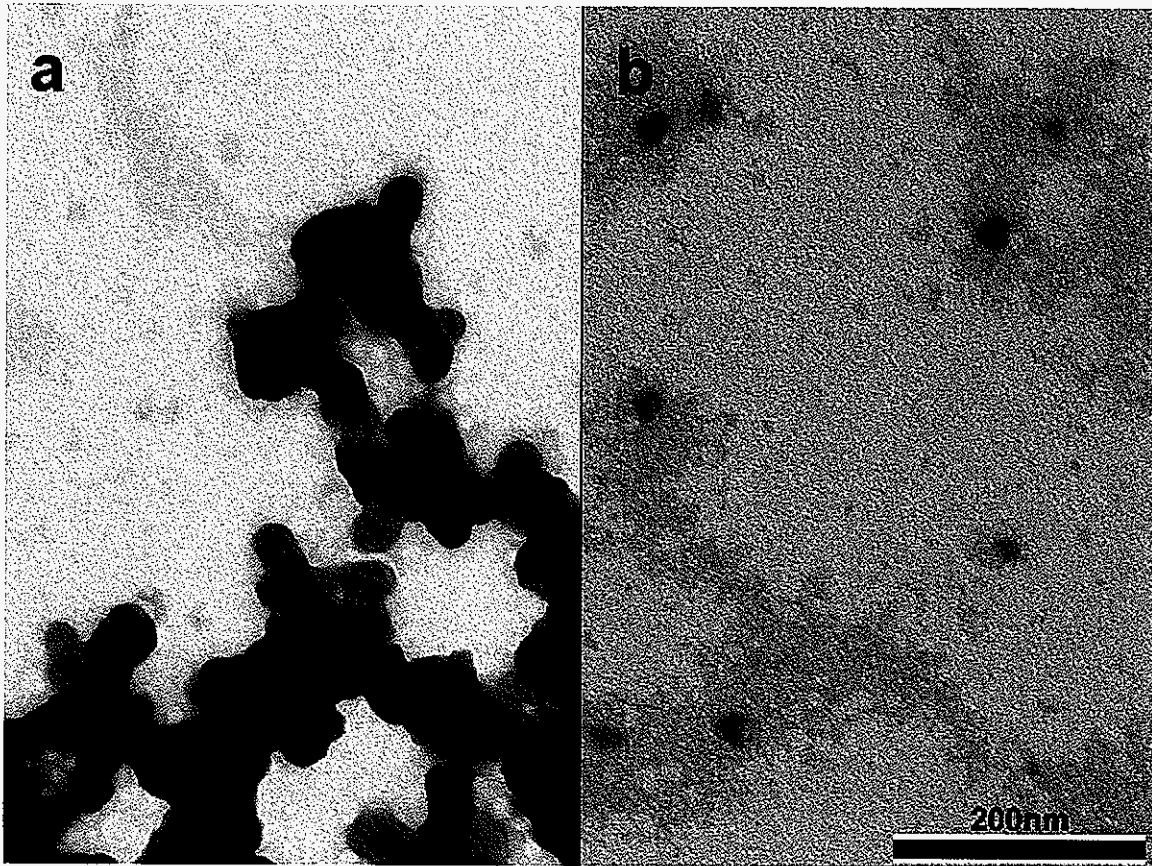


**Figure 7:** TEM of Dialyzed Sample a) agglomerated region b) disperse region

Formation of stable calcium phosphate inorganic phase, (Brushite and Monetite), was demonstrated by XRD and EDS. Stability of coated micelles was established by SAXS experiments. These particles showed constant radius of gyration,  $R_g$ , irrespective of the temperature indicating micelle geometry was retained even below critical micellation temperature as a result of the solid calcium phosphate coating. Transmission electron microscope images have shown that solid particles also remain intact after dialysis, more proof that the calcium phosphate coating protects the underlying polymer micelle.

While Zhao and Ma [1], propose a surfactant / inorganic precursor model to explain their mesoporous hydroxyapatite, Use of the modified pentablock polymer allows a more direct precipitation mechanism. The poly(2-dimethylaminoethyl methacrylate), PDEAEM end groups become highly protonated at low pH. This imparts cationic characteristics to the surface of the micelles, similar to Xu et al's thin film experiment [7, 10], and allows the ions in the solution to be attracted directly to the micelle surface.

### ***Acknowledgment***

Ames Laboratory is operated for the U.S. Department of Energy by Iowa State University under contract No. W-7405-ENG-82. This research was supported by the Department of Energy. The authors also wish to thank K. Schmidt-Rohr, A. Rawal, E. White, Y.E. Kalay, M. Kanapathipillai, C. Zhang, X. Wei, Y. Yusufoglu, and the people at Argonne National Lab.

### ***References***

1. Zhao, Y.F. and J. Ma, *Triblock co-polymer templating synthesis of mesostructured hydroxyapatite*. *Microporous and Mesoporous Materials*, 2005. **87**(2): p. 110-117.
2. Rusu, V.M., et al., *Size-controlled hydroxyapatite nanoparticles as self-organized organic-inorganic composite materials*. *Biomaterials*, 2005. **26**(26): p. 5414-5426.
3. Jonasova, L., et al., *Hydroxyapatite formation on alkali-treated titanium with different content of Na<sup>+</sup> in the surface layer*. *Biomaterials*, 2002. **23**(15): p. 3095-3101.
4. Jonasova, L., et al., *Biomimetic apatite formation on chemically treated titanium*. *Biomaterials*, 2004. **25**(7-8): p. 1187-1194.
5. Song, J., E. Saiz, and C.R. Bertozzi, *A new approach to mineralization of biocompatible hydrogel scaffolds: An efficient process toward 3-dimensional bonelike composites*. *Journal of the American Chemical Society*, 2003. **125**(5): p. 1236-1243.

6. Song, J., E. Saiz, and C.R. Bertozzi, *Preparation of pHEMA-CP composites with high interfacial adhesion via template-driven mineralization*. Journal of the European Ceramic Society, 2003. **23**(15): p. 2905-2919.
7. Xu, G., et al., *Biomimetic synthesis of macroscopic-scale calcium carbonate thin films. Evidence for a multistep assembly process*. Journal of the American Chemical Society, 1998. **120**(46): p. 11977-11985.
8. Determan, M.D., et al., *Synthesis and characterization of temperature and pH-responsive pentablock copolymers*. Polymer, 2005. **46**(18): p. 6933-6946.
9. Feigin, L.A. and D.I. Svergun, *Structure Analysis by Small-Angle X-Ray and Neutron Scattering*. 1 ed, ed. G.W. Taylor. 1987, New York: Plenum Press. 335.
10. Xu, G., I.A. Aksay, and J.T. Groves, *Continuous crystalline carbonate apatite thin films. A biomimetic approach*. Journal of the American Chemical Society, 2001. **123**(10): p. 2196-2203.

## **Chapter 3: Preparation of Tri-and Pentablock Polymer-Calcium Phosphate Gel Nanocomposites**

D. Enlow\*, A. Rawal\*\*, K. Schmidt-Rohr\*\*, S. Mallapragada\*\*\*, and M. Akinc\*

\* Materials Science and Engineering and Ames Laboratory \*\* Department of Chemistry and Ames Laboratory \*\*\* Department of Chemical Engineering and Ames Laboratory, Iowa State University, Ames Iowa.

### **Abstract**

Nanocomposite calcium phosphate-copolymer gels were prepared from aqueous solutions. NMR and WAXD showed that calcium phosphate precipitation in the Pluronic® F127 polymer gel resulted in a disordered brushite phase while the calcium phosphate-poly(2-diethylaminoethyl methacrylate) (PDEAEM) modified Pluronic® F127 pentablock polymer nanocomposite contained the same brushite phase along with a drying induced 25% crystalline calcium dihydrogen phosphate second phase. Using XRD, TGA, TEM, and NMR, it was confirmed that the calcium phosphate precipitated on and interacted with the polymer forming an agglomerated network of ~20 nm diameter nanospheres. The resulting polymer-calcium phosphate nanocomposites contained between 6.5 and 15 weight percent calcium phosphate, which could be controlled by manipulating the pH of the constituent solutions.

### *Introduction*

Because of their excellent biocompatibility, calcium phosphate based materials and coatings have been studied as potential implant materials. For example, brushite bone cements have been developed [1], and biomimetic apatite coatings for titanium and has been studied [2, 3]. Because calcium and phosphate are natural components in bone, many of these materials have improved bone bonding properties.

In addition to ceramics and coated metals, organic materials for medical implants have been studied as well. Muller et al investigated biomimetic apatite formation on chemically modified cellulose templates [4]. After treating highly oriented trimethylsilyether-cellulose (TMS-cellulose) fibers with a supersaturated  $\text{Ca}(\text{OH})_2$  solution, and exposing to simulated body fluid, Muller et al observed directed calcium phosphate precipitation on the surfaces of the cellulose fibers. With an initial diameter of about 20  $\mu\text{m}$ , these coated fibers reached a final diameter of over 90  $\mu\text{m}$ . After analyzing the electron diffraction patterns in TEM, it was found that the calcium phosphate precipitated as both octacalcium phosphate, and hydroxyl carbonated hydroxyapatite ( $\text{CO}_3\text{-HAp}$ ). This was supported by the strong calcium and phosphorous signals, and the Ca/P ratio was found to be 1.35 with EDS. The proposed mechanism for this was that the chemically treated active surfaces attracted ions from solution, which initiated precipitation.

Similarly, Song et al developed a procedure using poly(2-hydroxyethyl methacrylate) (pHEMA) hydrogel scaffolds [5, 6]. Like the cellulose in the previous study, Song et al were able to precipitate calcium phosphate onto the surface of hydrogel strips. In this case, urea

was used to slowly raise the solution pH and induce precipitation of calcium phosphate on the carboxylate-rich pHEMA surfaces. The result was a poorly crystalline ~5  $\mu\text{m}$  thick coating of hydroxyapatite over the surface of the hydrogel strip.

On a smaller scale, Rusu et al used chitosan as a natural biopolymer matrix for their hydroxyapatite nanoparticle composites [7]. By mixing calcium chloride and sodium dihydrogen phosphate with a solution of chitosan in water, they were able to show self-assembly and size control as the hydroxyapatite crystallites formed inside the chitosan matrix. Using this process at 22 °C, the initial product was nearly all brushite. This was converted to hydroxyapatite by raising the pH of the sample to the upper end of hydroxyapatite stability, making brushite a far less stable phase. They held the sample at this high pH and checked the phase with XRD at time intervals from 4 to 24 hours. Hydroxyapatite peaks begin to appear immediately after the pH is raised above 11 and is the dominant phase after 24 hours. Using XRD line broadening and TEM analysis, a bimodal crystallite size distribution was observed with 15-20 nm primary crystallites and larger “cluster-like” domains of 200-400 nm.

While all of these studies produce biomimetic polymer-ceramic composites, the polymer-ceramic interaction is limited for the most part to the surface of the polymer. With a similar process using a concentrated gel forming polymer, it should be possible to precipitate calcium phosphate throughout a network of agglomerated polymer nanospheres.

The Pluronic® F127 block copolymer, and the poly(2-diethylaminoethyl methacrylate) (PDEAEM) modified Pluronic® F127 pentablock polymer developed by Determan et al [8] self-assemble into micelles at low temperature and concentration in aqueous solutions, but these micelles agglomerate into a viscous gel at higher temperature or concentration. A temperature / concentration partial phase diagram of the pentablock polymer is shown in Figure 1.

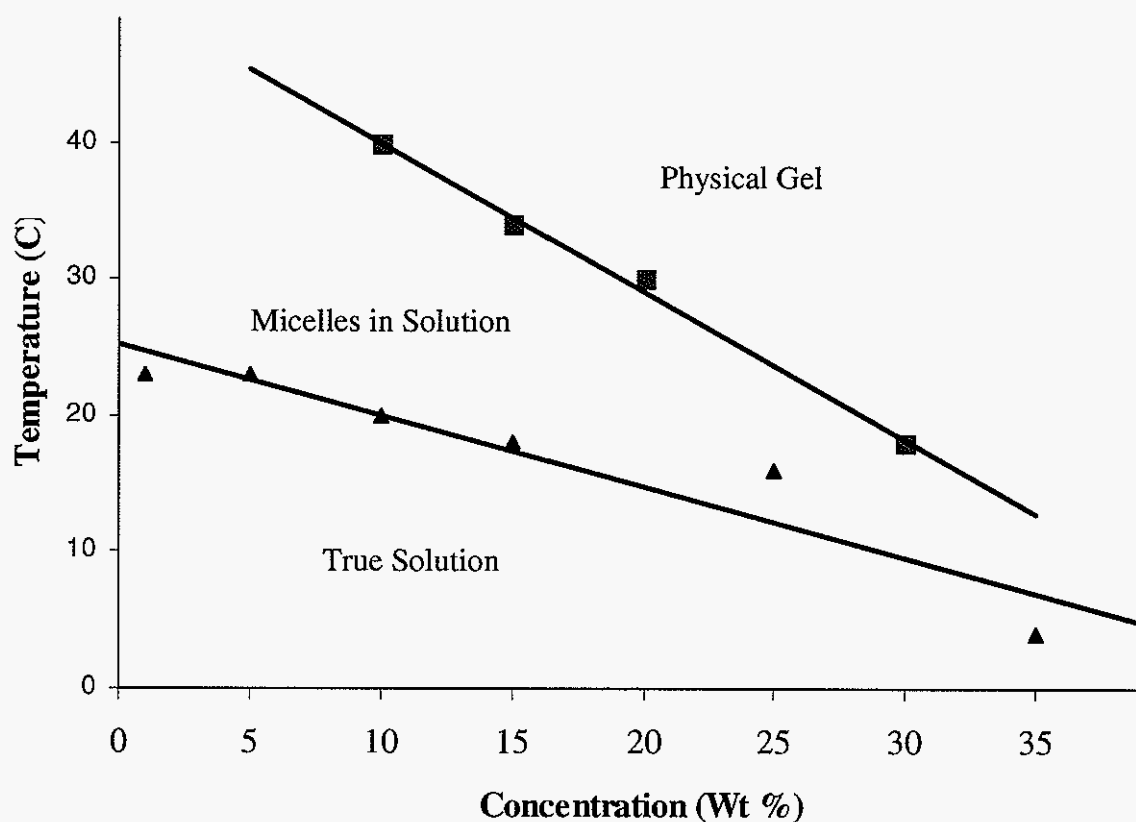


**Figure 1:** Temperature / concentration pentablock polymer phase transitions [8]

This temperature dependent transition makes it possible to combine the polymer and calcium phosphate components in solution, allowing for a homogeneous mixture of the micelle spheres and calcium phosphate. Where previous studies were limited to calcium phosphate-

polymer interaction on the surface of a bulk polymer, or fractions of a micron agglomerates of nanocomposites from solution, these polymers make it possible to precipitate calcium phosphate in the interstitial spaces between and on the surface of the concentrated spherical micelles within a macro-sized polymer gel.

### ***Materials and Methods***

Unless otherwise noted, all chemicals in this study were obtained from Fisher Scientific and are of laboratory grade and purity. Precipitation of calcium phosphate into the polymer gel matrix was achieved using aqueous solutions of ammonium dihydrogen phosphate ( $\text{NH}_4\text{H}_2\text{PO}_4$ ), phosphoric acid ( $\text{H}_3\text{PO}_4$ ), calcium nitrate ( $\text{Ca}(\text{NO}_3)_2$ ), and the PDEAEM modified pentablock polymer. A saturated solution of calcium phosphate with a Ca:P ratio of 1.67 as a stoichiometric hydroxyapatite was prepared by mixing 120 mL of a 0.5M solution of ammonium  $\text{NH}_4\text{H}_2\text{PO}_4$  with 200 mL of a 0.5M  $\text{Ca}(\text{NO}_3)_2$  solution. This solution was stirred for 30 minutes until a white precipitate formed. The mixture was then centrifuged and the clear supernatant was drawn off as the saturated calcium phosphate solution. This supernatant solution had a pH of 2.95.

A more concentrated solution was prepared by mixing 4.0M solutions of  $\text{H}_3\text{PO}_4$  and  $\text{Ca}(\text{NO}_3)_2$ . Sodium hydroxide (NaOH) was added until the solution reached a pH of 1.0 and a cloudy precipitate formed. Like the dilute solution described above, the supernatant was saved as the saturated calcium phosphate solution at pH=1.0.

Commercially available Pluronic® F127 (BASF Corporation, Florham Park, New Jersey) and the modified PDEAEM<sub>35</sub>-F127-PDEAEM<sub>35</sub> pentablock polymer developed by Determan et al [8] were used as the polymer matrix phase. Gel samples were prepared by dissolving 3 grams of the polymer directly into the Ca P solutions. Control samples of the polymer dissolved in deionized water were also prepared. These mixtures were placed in a refrigerator at 3°C and stirred daily until the polymer was completely dissolved. It took usually about 3 to 4 days to get a homogeneous solution. After dissolving, the samples were warmed to room temperature (22°C) and aged for 24 hours. During this time, as predicted by the temperature/concentration phase diagram shown in Figure 1, the calcium phosphate-polymer solution thickened into a viscous nanocomposite gel.

### *Characterization*

Because it was important to retain and analyze the aqueous structure of the polymer gel, Cryo-TEM was necessary. Gel samples were prepared as described above, placed onto bulls-eye stub, and frozen at -100°C in the chamber of a Reichert Ultracut S ultramicrotome with FCS cryo unit (Mager Scientific Inc., Dexter MI). Sections were made using a Diatome cryo-diamond knife (35°-dry; Electron Microscopy Sciences, Ft. Washington, PA) at 100nm and collected onto 300 mesh copper grids and placed into a grid transfer unit that was stored in liquid nitrogen until transferred to the TEM chamber. TEM samples were loaded into a liquid nitrogen cooled Gatan cold stage (Model 626DH, Gatan Inc. Pleasanton, CA) and imaged at 100kV in a Phillips CM 30 TEM (Phillips Corporation, Schaumburg, IL). Qualitative chemical analysis was done with a ThermoNoran EDS unit calibrated to its internal standards (Thermo Electron Corporation, Waltham, MA).

Structural characterization of the samples was accomplished by x-ray diffraction experiments using a theta-theta x-ray diffractometer (Scintag, XGEN-400, Cupertino, CA). Wet gel xrd samples were prepared and analyzed immediately to minimize drying. The Cu K $\alpha$  x-ray source was set to 45kV and 40mA, and the samples were scanned at a rate of 1°/min over a 2 $\theta$  range of 10° – 70°. Phase analysis was done using the ICDD database and the Scintag DMSNT search / match software.

Thermal gravimetric analysis (TGA) performed with a Perkin Elmer thermogravimetric analyzer (Perkin Elmer, TGA 7, Downers Grove IL). Approximately 40mg of the gel sample was placed in a platinum pan and the experiments were performed in a flowing air environment. The program was set to heat up to 100°C and hold at this temperature for 10 min, then heat from 100°C to 150°C at a rate of 3.00°C/min, and finally, heat from 150°C to 800°C at rate of 10°C/min.

The presence of water in solid-state NMR samples is undesirable since ionic currents lead to dissipation of radio-frequency power and can cause broadening of the probe-head tuning curve as well as sample heating. To prevent this, the samples were first dried by rotational evaporation and then lyophilized. For magic-angle-spinning NMR experiments, the samples were packed into 2.5-mm zirconia rotors with Kel-F caps. As desired, the probe head-tuning curve showed no significant broadening and the <sup>1</sup>H NMR spectrum was free of signals of loosely bound water.

All NMR experiments were carried out on a Bruker spectrometer (Bruker-Biospin DSX400, Rheinstetten, Germany) at 400 MHz for  $^1\text{H}$  and 162 MHz for  $^{31}\text{P}$  nuclei. A Bruker 2.5 mm double resonance magic-angle spinning (MAS) probehead, which enables short  $^1\text{H}$  and  $^{31}\text{P}$  pulses lengths of 2.5  $\mu\text{s}$  duration for a  $90^\circ$  flip angle, was used for 6.5 kHz MAS  $^1\text{H}$ - $^{31}\text{P}$  experiments. In direct-polarization (DP)  $^{31}\text{P}$  experiments, recycle delays of 400 s and 1000 s were used. In  $^1\text{H}$  and  $^1\text{H}$ - $^{31}\text{P}$  cross-polarization (CP) experiments, including two-dimensional (2D)  $^1\text{H}$ - $^{31}\text{P}$  wideline separation (WISE), recycle delays of 2 s were used before 400  $\mu\text{s}$  of Hartmann-Hahn cross-polarization (CP). The  $t_1$  increment was 20  $\mu\text{s}$ . Due to the presence of sharp peaks in the  $^1\text{H}$  spectrum, both cosine- and sine-modulated data were acquired to give the full frequency information in the  $^1\text{H}$  dimension.

Direct polarization (DP) and cross polarization (CP)  $^{31}\text{P}$  NMR spectra were acquired with  $^1\text{H}$  decoupling at 6.5 kHz MAS. The DP spectrum is quantitative if the recycle delay is sufficiently long. In order to ensure this, the DP experiments were run with increasing recycle delays until there was no further increase in signal intensity.  $^1\text{H}$ - $^{31}\text{P}$  CP experiments indicate the protonation state of the phosphate group, most pronouncedly after a short (< 500  $\mu\text{s}$ ) cross-polarization time. The comparison with the DP spectrum indicates whether there are non-protonated phosphates present, which cross polarize slowly or not at all. No Hahn spin echoes were used before detection because the transverse relaxation time of  $^{31}\text{P}$  in one sample (pluronic-based composite) was extremely short, possibly due to unfavorable proton dynamics in the phosphate.

All  $^1\text{H}$  NMR spectra were recorded at 6.5 kHz MAS using probe-head background suppression [9]. The line-width of the proton spectrum indicates the  $^1\text{H}$ - $^1\text{H}$  dipolar coupling, which increases with the proton density and decreases with the mobility of the segment. In rigid organic solids, the dipolar line width is  $\sim 40$  kHz.

Supramolecular proximities and domain sizes can be probed in NMR using  $^1\text{H}$  proton spin diffusion, during a “mixing” time  $t_m$  on the ms to 0.5-s time scale. During the evolution period of a two-dimensional experiment, the magnetization of protons in one phase (A) is modulated by its characteristic chemical-shift frequency  $\omega_A$ . If during  $t_m$  the magnetization diffuses to protons in a different phase (B), it will be detected with frequency  $\omega_B$ ; thus, domain proximity on the spin diffusion length scale (0.5 – 30 nm, depending on  $t_m$ ) results in an  $(\omega_A, \omega_B)$  cross peak in the two-dimensional spectrum. For small domain sizes, the equilibration is a fast process, while for large domains it is relatively slow. In the present case, phosphate protons are only a small percentage of the protons in the sample and therefore difficult to detect. Hence, we detect them indirectly, with excellent selectivity, in terms of  $^{31}\text{P}$  spins to which these protons cross-polarize.

The experiment with  $^1\text{H}$  evolution flanked by excitation and z-storage  $90^\circ$  pulses, spin diffusion time  $t_m$ , read-out pulse, cross polarization to  $^{31}\text{P}$ , and  $^{31}\text{P}$  detection effectively is a 2D WISE experiment [10]. At short  $t_m$ , the slice along the  $^1\text{H}$  dimension will reflect only the phosphate protons near the detected  $^{31}\text{P}$  spins; at longer  $t_m$  times, if there is spin diffusion contact between the phosphate protons and the protons from the surrounding polymer matrix,

the  $^1\text{H}$  lineshape will change to that of the polymer protons. This approach was previously demonstrated in polymer-clay nanocomposites using  $^1\text{H}$ - $^{29}\text{Si}$  WISE NMR by Hou et al [11].

### ***Results and Discussion***

Transmission electron microscopy of the pentablock gel prepared with the pH 1.0 calcium phosphate solution clearly indicated aggregates of spheres. The cryo-frozen gel appeared as a concentrated matrix of ~60 nm diameter spheres. That observation is consistent with the TEM analysis done by Determan et al [8] who observed 60-90 nm diameter total diameter spheres in a 3 wt% pentablock micelle solution. This micelle micrograph, as well as the 30 wt% pentablock in pH 1.0 calcium phosphate solution, is presented in Figure 2.

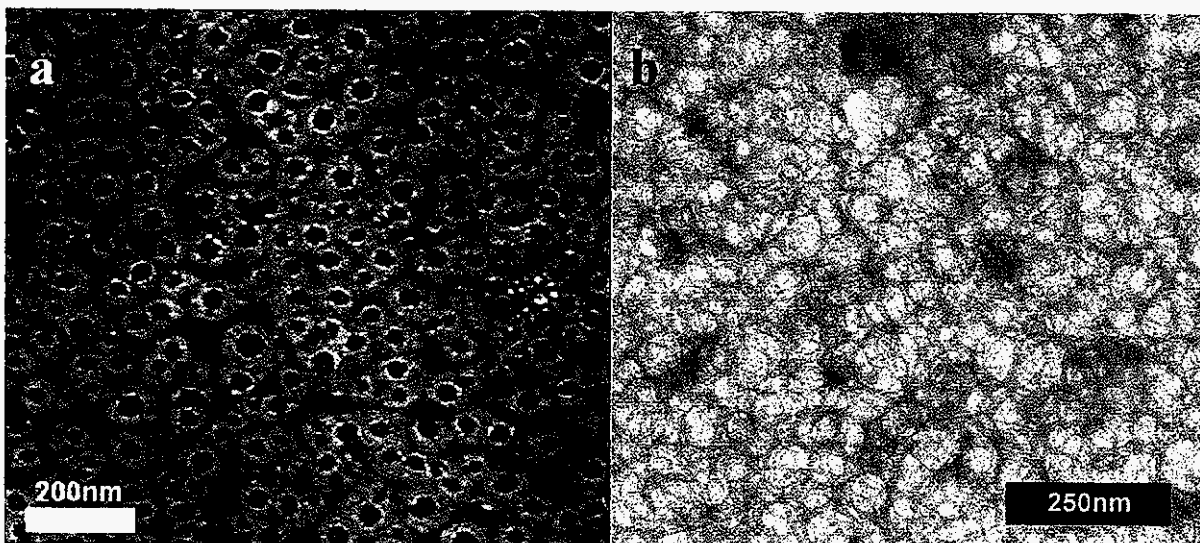


**Figure 2:** Cryo-TEM Micrographs of a) 3 wt % Pentablock Micelle Solution [8], and b) 30 wt% Pentablock-pH 1.0 Calcium Phosphate Gel [8]

While there is was no obvious visible second phase in the gel micrograph, EDS analysis showed strong Calcium and Phosphorous characteristic signals. This could be attributed to

the amorphous calcium and phosphate ions in solution, however, XRD results indicate crystalline brushite is present in this homogeneous aggregation of pentablock micelles.

The initial precipitate formed upon initial mixing of the 0.5M  $\text{Ca}(\text{NO}_3)_2$  and  $\text{NH}_4\text{H}_2\text{PO}_4$  aqueous solutions showed a mixture of synthetic brushite ( $\text{CaPO}_3(\text{OH}) \cdot 2\text{H}_2\text{O}$ ) and monetite ( $\text{CaPO}_3(\text{OH})$ ). XRD of the precipitate formed in the gel samples show a similar but different inorganic phase. When precipitated on the polymer gel template, natural brushite, a mineral normally only found in caves was observed [12]. Figure 3 presents x-ray diffraction patterns of both the Pluronic® F127 and pentablock gels dissolved in deionized water and in the pH 2.95 Ca P solution, as well as the characteristic peaks of natural brushite (ICDD card # 11-0293). Figures 3 a and b do not show any sharp peaks, only amorphous reflections of the non-crystalline polymers. The pH 2.95 gel samples in Figures 3 c and d, however, show all 5 of natural brushite's most intense peaks. The natural brushite characteristic peaks are also presented as Figure 3e.

Like the precipitate separated upon initial mixing of the calcium phosphate solutions, X-Ray analysis of the higher ionic concentration pH 1.0 gel samples showed the synthetic brushite phase. Because the solution was much more concentrated, there was more of a driving force for precipitation on the polymer. This led to less controlled precipitation and formation of the synthetic phase. After drying for 24 hours in a desiccator, a second phase formed. Along with the now synthetic brushite peaks, calcium dihydrogen phosphate was also present. XRD patterns of the pH 1.0 pentablock gel and the same dried sample are presented in Figure 4. As the water evaporated from the sample, ions formerly in solution were forced to

precipitate. Because of the now overwhelming driving force, ions precipitated heterogeneously as a second phase. Curiously, this second phase was not present in the pH 1.0 Pluronic® F127 gel.

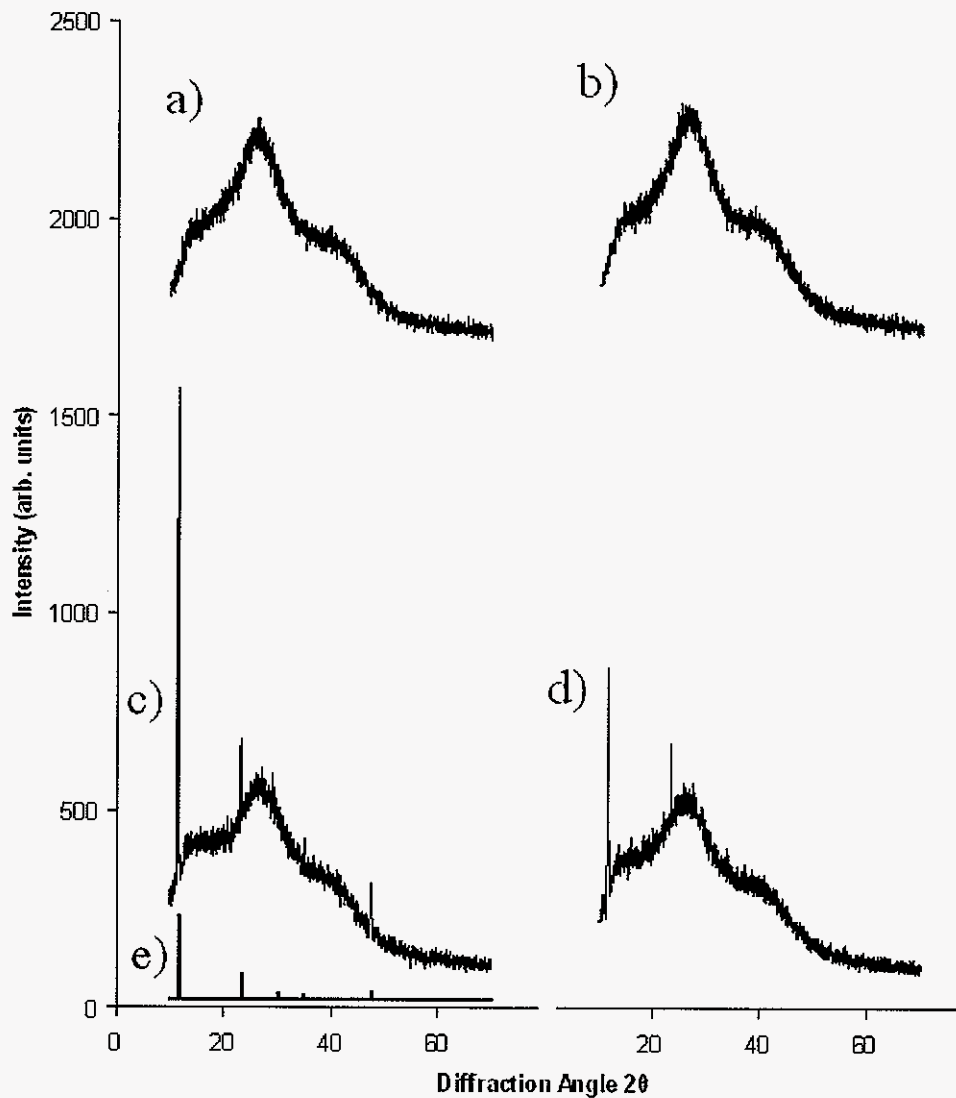


**Figure 3:** X-Ray Diffraction Patterns of a) 30 wt% pentablock in deionized water, b) 30 wt% Pluronic® F127 in deionized water, c) 30 wt% pentablock in pH 2.95 Ca P solution, d) 30 wt% Pluronic® F127 in pH 2.95 Ca P solution, and e) Characteristic natural brushite peaks.

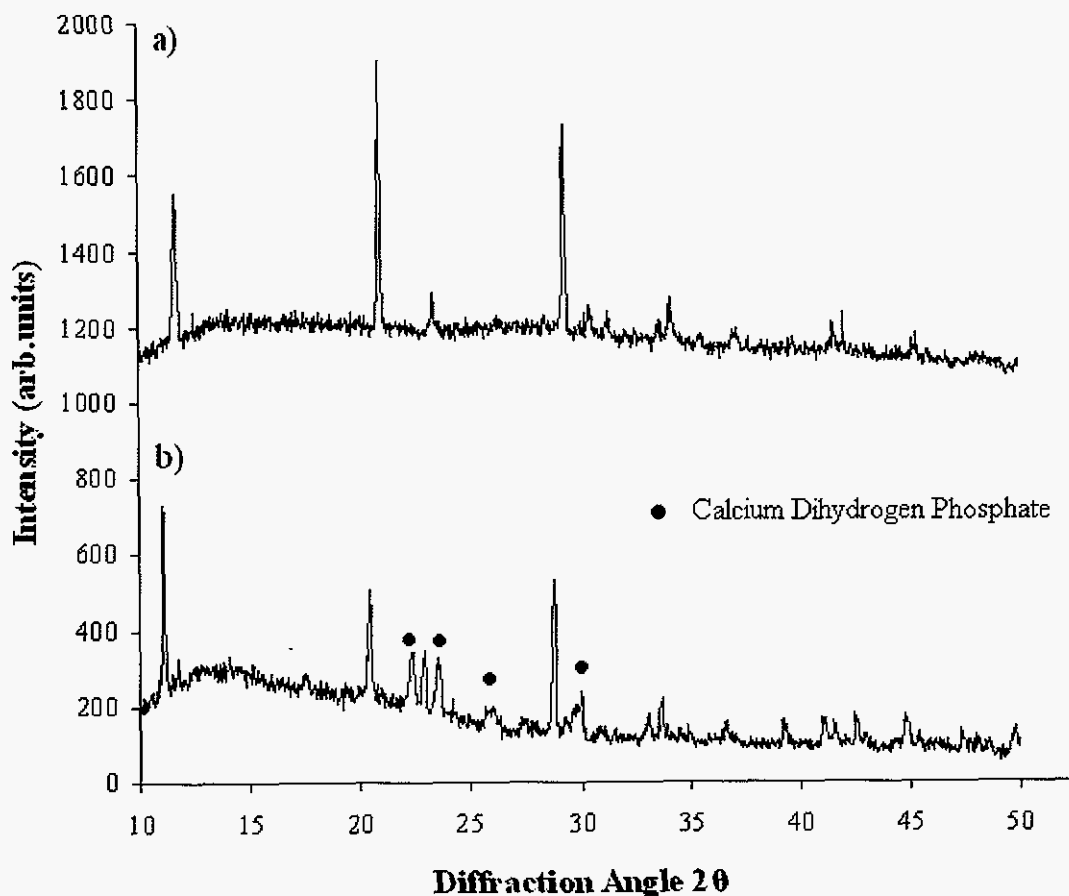


**Figure 4:** X-Ray diffraction patterns of a) 30 wt% pentablock gel in pH 1.0 calcium phosphate solution, and b) same sample after 24 hours drying in a desiccator.

It was possible to control the amount of precipitation by adjusting the pH of the initial calcium phosphate solution. TGA of the pH 2.95 and pH 1.0 samples illustrated this. After evaporating all the water out of the gel, a baseline weight was found for each sample. Because of the chemically bound water from the brushite phase, water was not totally evaporated until the system reached 200°C. At 400°C, after burning out all of the polymer, it

was found that in the pH 2.95 gel, 6.5 % of the solid phase was calcium phosphate. As predicted by the pH solubility diagrams [13], the inorganic weight % in the pH 1.0 gel sample was much higher at 15.0 %. Using this data, it was also possible to calculate out the initial concentrations of the calcium phosphate solutions. Assuming all of the left over precipitate is the dehydrated monetite phase, it was determined that the initial calcium and phosphate concentrations were 0.5 M in the pH 1.0 and 0.2 M in the pH 2.95 calcium phosphate solutions. Considering the 40 mg size of the samples, these experimentally calculated concentrations are consistent with the theoretical pH concentration diagram of the calcium phosphate system [13]. The TGA results are shown in Figure 5.

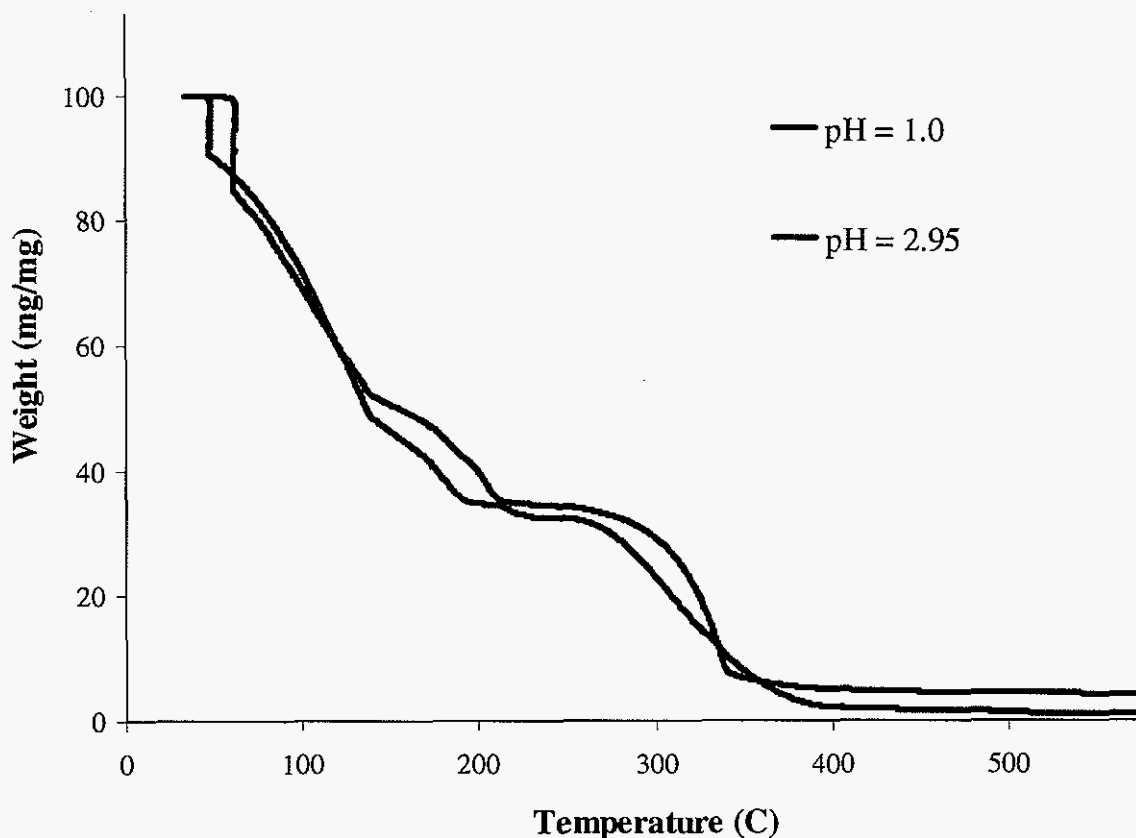


**Figure 5:** TGA of 30 wt% Pentablock Polymer Gel dissolved in Ca P Solution

The  $^{31}\text{P}$  NMR spectra of the Pluronic® F127 - and pentablock – phosphate composites are shown in Figure 6. Comparing the cross-polarization to the direct-polarization spectra, in both instances, we see that the same peaks are present in both spectra, and with almost equal intensities for the Pluronic® F127- phosphate composite. This indicates that all the phosphates exist as protonated species. For the Pluronic® F127 phosphate, the resonance is indicative of a brushite / monetite phase ( $\text{CaHPO}_4$  with or without water of crystallization), while the pentablock phosphate contains a significant contribution (ca. 1/3 of all phosphate) from calcium dihydrogen phosphate (CaDHP). For reference, the spectrum of pure CaDHP is shown in Figure 6e; it exhibits two signals due to chemically inequivalent  $\text{H}_2\text{PO}_4^-$  ions in the crystal structure. The Pluronic® F127-phosphate has a broader line shape as compared to the pentablock-phosphate, which suggests that the former exists in a more disordered environment. The spectra in Figure 6 have been scaled to equal peak height, but the true integrals of the spectra in Figure 6a and 5c indicate ca. five times more phosphate in the pentablock composite as compared to the Pluronic® F127 composite, given the almost equal fill factor in both sample rotors.

Furthermore, the CaDHP has a roughly twice longer  $^{31}\text{P}$  longitudinal ( $T_1$ ) relaxation time as compared to the  $\text{CaHPO}_4$ , which indicates that there is no efficient  $^{31}\text{P}$  spin diffusion between the two phosphates on the 1-s time scale. This in turn means that the two phases are not in contact with domains on the 2-nm scale.

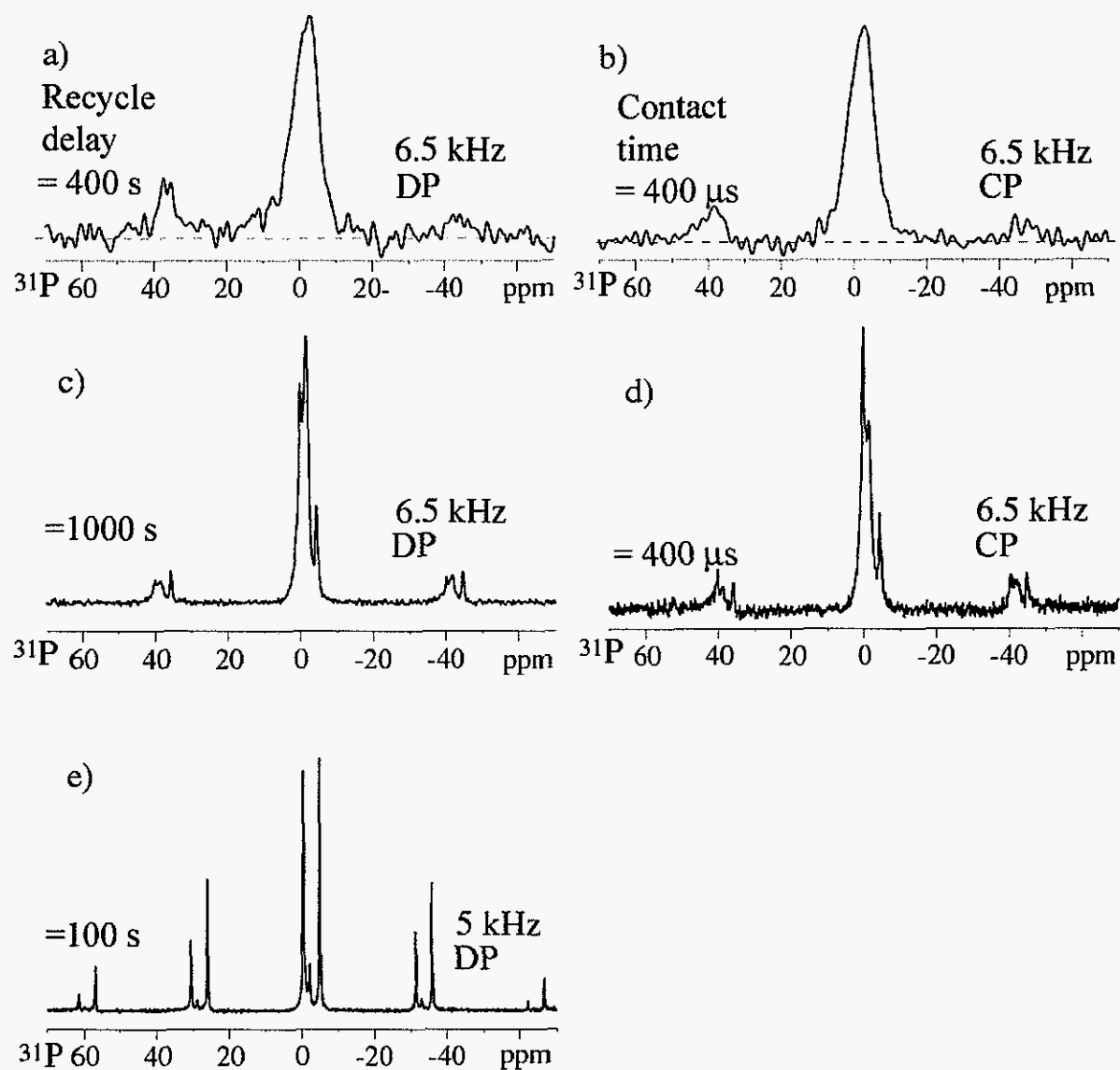


**Figure 6:**  $^{31}\text{P}$  NMR spectra of (a, b) a Pluronic® F127-phosphate composite, (c, d) pentablock-phosphate composite, and (e) calcium dihydrogen phosphate.

The  $^1\text{H}$  proton spectra of the Pluronic® F127 composite are shown in Figure 7. The sharp resonances from the Pluronic® protons dominate the spectrum in the pentablock composite as well. Normally, in organic solid the proton resonances are very broad due to the strong multi-spin  $^1\text{H}$ - $^1\text{H}$  dipolar couplings. However, fast segmental motion above the glass

transition averages out the dipolar interactions in the Pluronic® F127 polymer, resulting in the sharp lines seen in Figure 7. The proton spectrum of the Pluronic® F127 composite shows a broad component (Figure 7 c, d), which may be due to the reduced mobility of the Pluronic® F127 segments near the brushite particles.

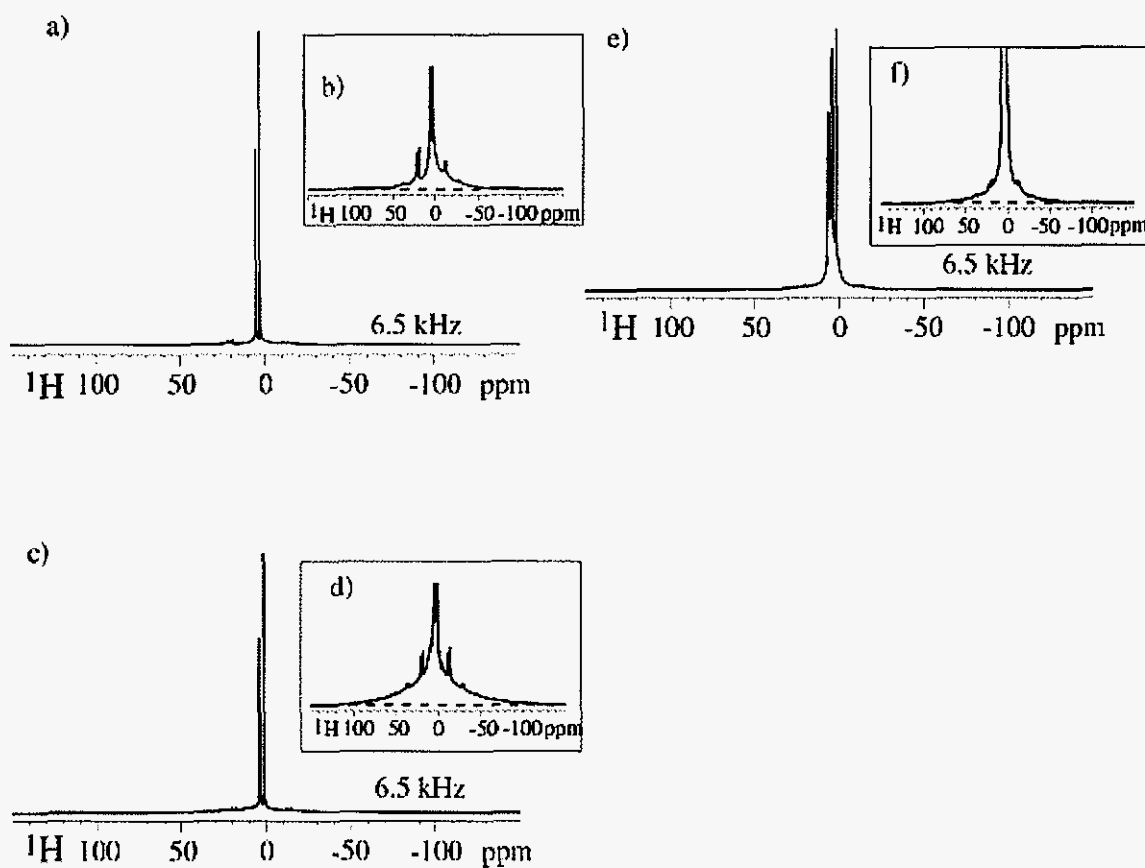


**Figure 7:**  $^1\text{H}$  NMR spectrum of (a, b) the pure Pluronic® F127, (c, d) the Pluronic® F127 - phosphate composite, and (e, f) the pentablock-phosphate composite at 6.5 kHz MAS. The insets (b), (d), and (f) focus in on the base of their respective spectra, revealing a broadened base of the pluronic-phosphate composite.

$^1\text{H}$ - $^{31}\text{P}$  WISE proved useful for characterizing the proximity of the inorganic components to the organic matrix. As seen in the WISE spectra of Figure 8, for the Pluronic® F127 composite,  $^1\text{H}$  spin diffusion from the pluronic to the brushite protons occurs within 50 ms of spin diffusion time, as proved by the characteristic sharp doublet of the pluronic protons clearly visible after 50 ms of spin diffusion. Given a spin diffusion coefficient of  $< 0.5 \text{ nm}^2/\text{ms}$  in protonated phosphates, this indicates domain sizes of less than 20 nm.

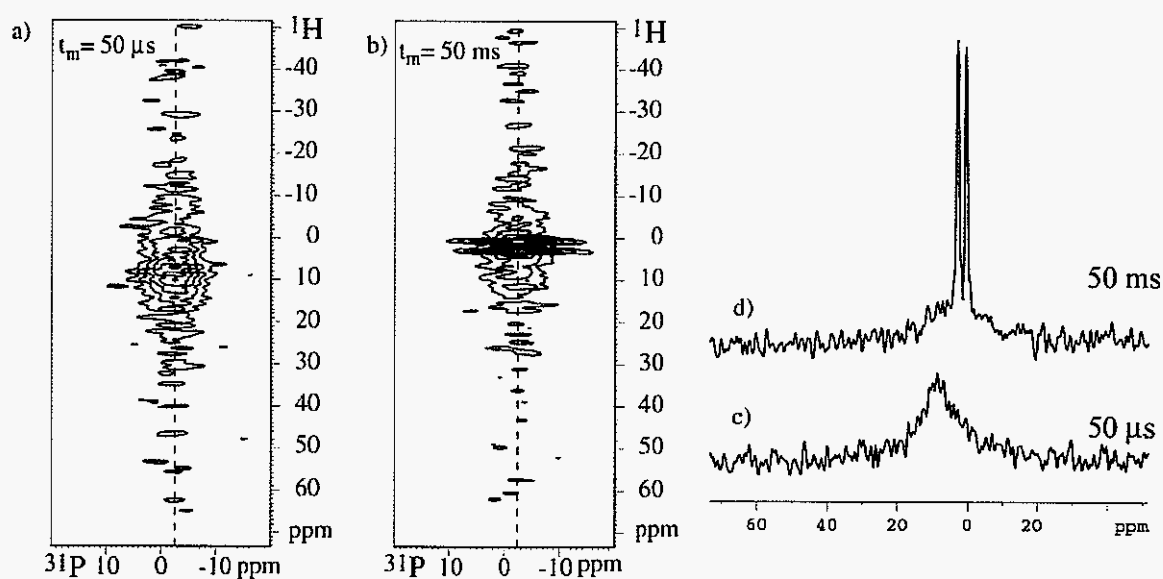


**Figure 8:**  $^1\text{H}\{^{31}\text{P}\}$  2D WISE at 6.5 kHz MAS of the Pluronic® F127–phosphate composite. (a) and (b) are 2D contour plots of spectra recorded after 0.05 and 50 ms of spin diffusion, respectively. Figures (c) and (d) are slices along the  $^1\text{H}$  dimension extracted at 1.6 ppm in the  $^{31}\text{P}$  dimension from the spectra in (a) and (b), respectively.

In contrast, there is hardly any evidence of spin diffusion contact in the case of the pentablock composite, see Figure 9. After 50 ms of spin diffusion, little line-shape change is observed, see Figure 9 b, e. The characteristic doublet of the Pluronic® F127 block is absent. Only a minor signal in the 1 – 8 ppm range might be attributed to the polymer

protons. This indicates large particles > 20 nm in diameter, where most of the protons are far away from the pentablock matrix. No signs of spin diffusion, only signal reductions by  $^1\text{H}$   $T_1$  relaxation, are observed after 500 ms, see Figure 9c, f.

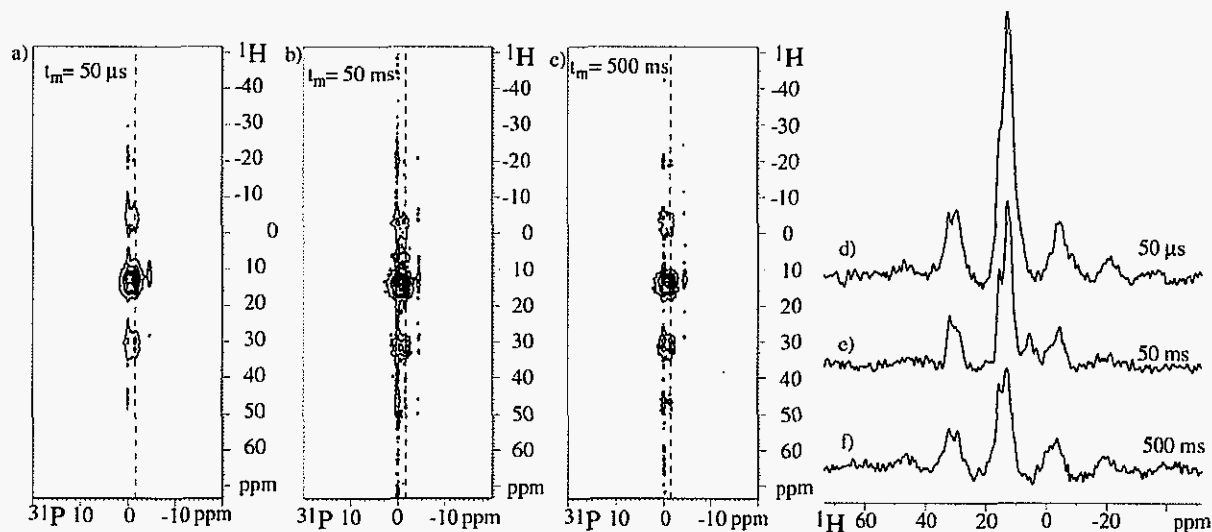


**Figure 9:**  $^1\text{H}$   $\{^{31}\text{P}\}$  2D WISE at 6.5 kHz MAS of the pentablock–phosphate composite. (a), (b) and (c), are 2D contour plots of spectra recorded after 50  $\mu\text{s}$ , 50 ms and 500 ms of spin diffusion respectively. Figures (d), (e) and (f) are slices extracted along the  $^1\text{H}$  dimension from (a), (b), and (c), respectively, indicated by the dashed lines corresponding to 1.6 ppm in the  $^{31}\text{P}$  dimension.

### Conclusion

Like the lower concentration pentablock polymer micelle work done, calcium phosphate nucleation occurs on the pentablock polymer micelle surface because of the cationic characteristics given by the PDEAEM end groups. As micelles these hydrophilic end groups align themselves into a continuous cationic spherical surface. This attracts the ions in solution and provides sites for nucleation. A similar mechanism provides nucleation sites in the Pluronic® F127 gel. Pluronic® F127 micelles have polar OH end groups that when

assembled as a surface provide slightly negatively charged sites for nucleation. Because of the high concentration of polymer in the gel samples, at temperatures above 5°C, the micelles agglomerate into a nano-composite network.

The  $^{31}\text{P}$  1-D NMR identifies the phosphate in the Pluronic® F127 composite as a disordered brushite type species and that in the pentablock composite is relatively more ordered and contains ca. 25% of crystalline calcium dihydrogen phosphate. It also shows that there is more mineral content in the pentablock composite as compared to the pluronic composite. The  $^1\text{H}$ - $^{31}\text{P}$  WISE experiments with  $^1\text{H}$  spin diffusion showed that the brushite particles in the pluronic matrix are < 20 nm in diameter, while the CaDHP particles in the pentablock system are larger (>20 nm). The NMR data supports x-ray diffraction and TEM indications of a second calcium dihydrogen phosphate phase that forms during drying.

While most previous work has focused on mineralizing the surface of bulk polymers [4-6] samples or forming sub-micron aggregates of organic-inorganic nanocomposites [7, 14], use of gel forming self assembling polymers makes possible the formation of macro-sized networks of spherical nanocomposites.

### ***Acknowledgment***

Ames Laboratory is operated for the U.S. Department of Energy by Iowa State University under contract No. W-7405-ENG-82. This research was supported by the Department of Energy. The authors also wish to thank M. Kanapathipillai, E. White, Y.E. Kalay, Y. Yusufoglu, X. Wei, M. Kramer and O. Ugurlu.

## References

1. Malsy, A. and M. Bohner, *Brushite conversion into apatite*. European Cells and Materials, 2005. **10**(Suppl. 1): p. 28.
2. Jonasova, L., et al., *Hydroxyapatite formation on alkali-treated titanium with different content of Na<sup>+</sup> in the surface layer*. Biomaterials, 2002. **23**(15): p. 3095-3101.
3. Jonasova, L., et al., *Biomimetic apatite formation on chemically treated titanium*. Biomaterials, 2004. **25**(7-8): p. 1187-1194.
4. Muller, F.A., et al. *Biomimetic Apatite Formation on Chemically Modified Cellulose Templates*. in *The Annual Meeting of the International Society for Ceramics in Medicine, Nov 6-9 2003*. 2004. Porto, Portugal: Trans Tech Publications Ltd.
5. Song, J., E. Saiz, and C.R. Bertozzi, *A new approach to mineralization of biocompatible hydrogel scaffolds: An efficient process toward 3-dimensional bonelike composites*. Journal of the American Chemical Society, 2003. **125**(5): p. 1236-1243.
6. Song, J., E. Saiz, and C.R. Bertozzi, *Preparation of pHEMA-CP composites with high interfacial adhesion via template-driven mineralization*. Journal of the European Ceramic Society, 2003. **23**(15): p. 2905-2919.
7. Rusu, V.M., et al., *Size-controlled hydroxyapatite nanoparticles as self-organized organic-inorganic composite materials*. Biomaterials, 2005. **26**(26): p. 5414-5426.
8. Determan, M.D., et al., *Synthesis and characterization of temperature and pH-responsive pentablock copolymers*. Polymer, 2005. **46**(18): p. 6933-6946.
9. Chen, Q., S.S. Hou, and K. Schmidt-Rohr, *A simple scheme for probehead background suppression in one-pulse <sup>1</sup>H NMR*. Solid State Nuclear Magnetic Resonance, 2004. **26**(1): p. 11-15.
10. Schmidt-Rohr, K., J. Clauss, and H.W. Spiess, *Correlation of structure, mobility, and morphological information in heterogeneous polymer materials by two-dimensional wideline-separation NMR spectroscopy*. Macromolecules, 1992. **25**(12): p. 3273-3277.
11. Hou, S.S., F.L. Beyer, and K. Schmidt-Rohr, *High-sensitivity multinuclear NMR spectroscopy of a smectite clay and of clay-intercalated polymer*. Solid State Nuclear Magnetic Resonance, 2002. **22**(2-3): p. 110-127.
12. Murray, J. and R. Dietrich, *Brushite and Taranakite from Pig Hole Cave, Giles County, Virginia*. American Mineralogist, 1956. **41**: p. 616-626.
13. Oonishi, H. and K. Oomamiuda, eds. *Degradation/resorption in bioactive ceramics in orthopaedics*. First ed. Handbook of Biomaterial Properties, ed. J. Black and G. Hastings. 1998, Chapman and Hall: London. 590.
14. Zhao, Y.F. and J. Ma, *Triblock co-polymer templating synthesis of mesostructured hydroxyapatite*. Microporous and Mesoporous Materials, 2005. **87**(2): p. 110-117.

## Chapter 4: General Conclusions

### *Summary*

Biomimetic nanocomposites of calcium phosphate and self-assembling tri- and pentablock copolymers were produced. Pluronic® F127, and a pentablock polymer produced by grafting blocks of poly(diethylaminoethyl methacrylate) (PDEAEM) blocks to the ends of the Pluronic® F127 were mixed with pH 1.0 and pH 2.95 solutions of calcium phosphate resulting in brushite coated polymer micelles and gel. Analysis with TEM and EDS showed nucleation and growth of calcium phosphate on the micelles, and with XRD it was determined that brushite formed. These 40 nm diameter coated micelles retained their shape after diluting or decreasing the temperature to points below the critical micellation points, which proved that the inorganic coating imparts stability to the micelles.

Gel samples consisted of similar 60 nm diameter coated micelles packed together in to a matrix. Indicated by TEM and XRD, brushite precipitated homogeneously on and around the sphere surfaces. Solid-state NMR confirmed the presence of a polymer-disordered brushite single phase nanocomposite.

### *Conclusions*

Biomimetic nanocomposites of brushite and a PDEAEM modified Pluronic® F127 copolymer have been produced. Already concentration and temperature sensitive, addition of PDEAEM end groups imparts cationic characteristics and pH sensitivity. When

assembled into micelles, this produces a negatively charged surface and provides low energy nucleation sites for mineral deposition.

Pluronic® F127 nanocomposites form by a similar mechanism. When assembled into micelles, the polar OH end groups align and produce a slightly negatively charged surface. Like with the pentablock polymer, this surface provides sites for nucleation.

Having shown stability in varying conditions and strong polymer-calcium phosphate interactions, the self-assembling micelle and gel forming Pluronic® F127 and PDEAEM modified Pluronic® F127 polymers show a lot of promise as potential biomimetic materials and further work should be done to explore their potential.

### ***Future Research***

Future work should focus on controlling the calcium phosphate phase precipitating in the nanocomposites. While some brushite is present in the body, and has some applications as an implant material, hydroxyapatite is a much closer match to bone, and has many more biomedical applications.

To precipitate hydroxyapatite instead of brushite, the experiment must be carried out at a much higher pH. This however has the negative effect of decreasing the calcium and phosphate solubility in aqueous solutions. Because of this, one cannot simply increase the pH of the calcium phosphate solution before mixing with the polymer. While this should result in hydroxyapatite precipitation, the amount would be too small to detect with XRD,

EDS, or NMR. A similar problem occurs when the pH of an already mixed calcium phosphate-polymer micelle solution is raised by addition of base externally. Addition of a strong base causes uncontrolled local supersaturation and homogeneous precipitation of a second phase.

Because of these issues, pH needs to be raised slowly and uniformly throughout the solution. Thermo-decomposition of urea, for example, can raise the pH of a solution slowly and homogeneously. Another technique could be using calcium complexes to lock up calcium in the solution. Environmental conditions like temperature or radiation could then be used to break down the complex and release calcium into the system for slow and controlled precipitation of hydroxyapatite.